การจำลองการปลูกฟิล์มบางแบบโมเลกุลาร์บีมเอพิแทกซีที่เกิดตำหนิแบบช่องว่าง

นายณรงค์ จันทร์เล็ก

สถาบันวิทยบริการ
จุฬาลงกรณ์มหาวิทยาลัย

วิทยานิพนธ์นี้เป็นส่วนหนึ่งของการศึกษาตามหลักสูตรปริญญาวิทยาศาสตรมหาบัณฑิต

สาขาวิชาฟิสิกส์ ภาควิชาฟิสิกส์

คณะวิทยาศาสตร์ จุฬาลงกรณ์มหาวิทยาลัย

ปีการศึกษา 2548

ISBN 974-17-4335-1

ลิขสิทธิ์ของจุฬาลงกรณ์มหาวิทยาลัย

MODELLING OF MOLECULAR BEAM EPITAXY THIN FILM GROWTH
WITH VOID DEFECT FORMATION

Mr. Narong Chanlek

สถาบันวิทยบริการ
จุฬาลงกรณ์มหาวิทยาลัย

A Thesis Submitted in Partial Fulfillment of the Requirements
for the Degree of Master of Science Program in Physics
Department of Physics
Faculty of Science
Chulalongkorn University
Academic year 2005
ISBN 974-17-4335-1

Thesis Title	Modelling of Molecular Beam Epitaxy Thin Film Growth with Void Defect Formation
By	Mr. Narong Chanlek
Field of Study	Physics
Thesis Advisor	Assistant Professor Patcha Chatraphorn, Ph.D.
Thesis Co-Advisor	Nakorn Phaisangittisakul, Ph.D.

Accepted by the Faculty of Science, Chulalongkorn University in Partial Fulfillment of the Requirements for the Master's Degree

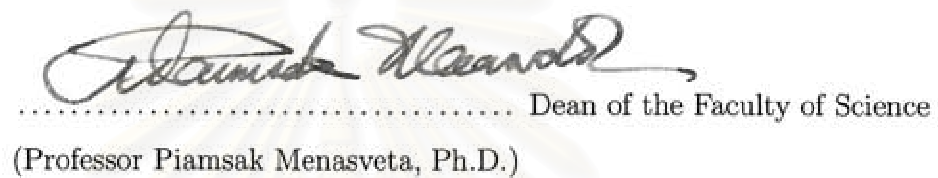

.... Dean of the Faculty of Science

(Professor Piamsak Menasveta, Ph.D.)

THESIS COMMITTEE

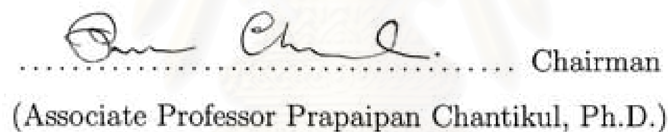

.... Chairman

(Associate Professor Prapaipan Chantikul, Ph.D.)

.... Thesis Advisor

(Assistant Professor Patcha Chatraphorn, Ph.D.)

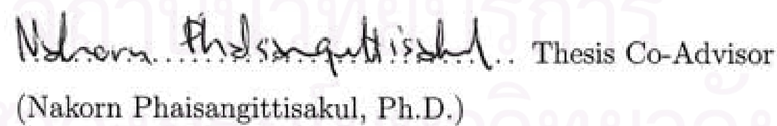

.... Thesis Co-Advisor

(Nakorn Phaisangittisakul, Ph.D.)

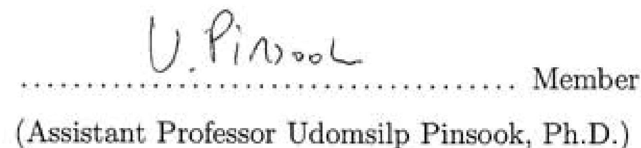

.... Member

(Assistant Professor Udomsilp Pinsook, Ph.D.)

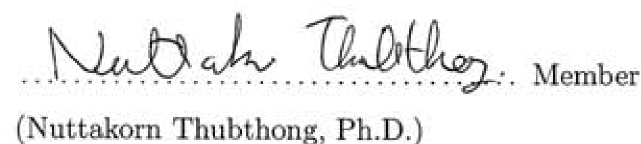

.... Member

(Nuttakorn Thubthong, Ph.D.)

สถาบันวิทยบริการ
จุฬาลงกรณ์มหาวิทยาลัย

ณรงค์ จันทร์เล็ก : การจำลองการปลูกฟิล์มบางแบบโมเลกุลาร์บีมเอพิแทกซีที่เกิดตำหนิแบบช่องว่าง. (MODELLING OF MOLECULAR BEAM EPITAXY THIN FILM GROWTH WITH VOID DEFECT FORMATION) อ. ที่ปรึกษา : ผศ. ดร. ปัจฉา ฉัตราภรณ์, อ.ที่ปรึกษาร่วม : ดร. นคร ไพศาลกิตติสกุล, 65 หน้า. ISBN 974-17-4335-1.

การปลูกฟิล์มบางแบบโมเลกุลาร์บีมเอพิแทกซี (เอ็มบีอี) ได้มีการศึกษาอย่างแพร่หลายเนื่องจากการประยุกต์ใช้งานทางเทคโนโลยีด้านอุปกรณ์สารกึ่งตัวนำ ในงานนี้ได้ใช้แบบจำลอง 2 แบบเพื่อศึกษาการปลูกฟิล์มแบบเอ็มบีอีในกรณีที่มีตำหนิแบบช่องว่างเกิดขึ้น แบบจำลองนี้คือ Random Deposition (RD) model with thermal activation และ Ballistic Deposition (BD) model with thermal activation ในแบบจำลอง RD model with thermal activation กฎการตกสะสมเป็นไปตามเงื่อนไขแบบ Solid-On-Solid (SOS) นั่นคือไม่อนุญาตให้เกิดช่องว่างในเนื้อสาร การห้อยของตัวอะตอม และการคาย สำหรับแบบจำลอง BD model with thermal activation ไม่ได้จำกัดเงื่อนไขแบบ SOS ในกระบวนการตกสะสม กระบวนการแพร่ในกรณีที่อะตอมสามารถแพร่ได้อย่างต่อเนื่องโดยปราศจากเงื่อนไขแบบ SOS สามารถเกิดขึ้นได้ในทั้งสองแบบจำลอง จากแบบจำลองเหล่านี้เราพบว่าอุณหภูมิของแผ่นรองรับมีผลอย่างมากต่อรูปร่าง, ความหนาแน่นของตำหนิแบบช่องว่างและความขรุขระของฟิล์ม ในแบบจำลอง RD model with thermal activation พบว่าการปลูกฟิล์มสามารถแบ่งได้ 2 ช่วง ในช่วงแรก อุณหภูมิมีค่าต่ำดังนั้นอะตอมบนพื้นผิวมีโอกาสในการแพร่ต่ำ เป็นผลให้ฟิล์มมีลักษณะขรุขระมากและความหนาแน่นของตำหนิแบบช่องว่างเพิ่มขึ้นตามค่าของอุณหภูมิ รวมทั้งความขรุขระของฟิล์มเพิ่มขึ้นอย่างรวดเร็ว ช่วงที่สอง ที่อุณหภูมิสูงขึ้น ฟิล์มมีลักษณะเรียบและความหนาแน่นของตำหนิแบบช่องว่างมีค่าลดลงเมื่ออุณหภูมิมีค่าเพิ่มขึ้น ความขรุขระของฟิล์มเพิ่มขึ้นอย่างช้าๆ ในแบบจำลอง BD model with thermal activation ฟิล์มจะมีลักษณะเรียบและ ความหนาแน่นของตำหนิแบบช่องว่างจะมีค่าลดลงในขณะเดียวกันความขรุขระของฟิล์มจะเพิ่มขึ้นช้าลง เมื่ออุณหภูมิของแผ่นรองรับมีค่าเพิ่มขึ้น

สถาบันวิทยบริการ
จุฬาลงกรณ์มหาวิทยาลัย

ภาควิชา.........ฟิสิกส์.....	ลายมือชื่อนิสิต........ณรงค์ จันทร์เล็ก........
สาขาวิชา.......ฟิสิกส์.....	ลายมือชื่ออาจารย์ที่ปรึกษา........[signature]........
ปีการศึกษา....2548......	ลายมือชื่ออาจารย์ที่ปรึกษาร่วม Nakorn Phaisangittisakul

4672258123 :MAJOR PHYSICS

KEY WORDS: VOID DEFECT / RD MODEL / BD MODEL / MBE GROWTH

NARONG CHANLEK : MODELLING OF MOLECULAR BEAM EPITAXY THIN FILM GROWTH WITH VOID DEFECT FORMATION. THESIS ADVISOR : ASST. PROF. PATCHA CHATRAPHORN, PH.D., THESIS COADVISOR : NAKORN PHAISANGITTISAKUL, PH.D., 65 pp. ISBN 974-17-4335-1.

Molecular beam epitaxy (MBE) thin film growth is widely studied due to its applications in semiconductor devices technology. In this work, we use two discrete models to study the MBE growth in which void defect can be formed. These discrete models are Random Deposition (RD) model with thermal activation and Ballistic Deposition (BD) model with thermal activation. In the RD model with thermal activation, the deposition rule obeys Solid-On-Solid (SOS) condition: bulk vacancy, overhanging of an atom and desorption are not permitted. In the BD model with thermal activation, the SOS condition is not restricted in the deposition process. The diffusion process in which surface atoms can diffuse continuously without the SOS condition is possible in both models. From these models, we found that the substrate temperature has strong effect on morphology, void defect density and roughness of the film. In the RD model with thermal activation, the growth can be divided into two regimes. In the first regime, the temperature is low so the surface atom has low probability to diffuse. As a result, the film is very rough and the void defect density increases with the temperature. The roughness increases rapidly. In the second regime, at higher temperature, the film becomes smooth and the void defect density decreases as the temperature increases. The roughness increases slowly. In the BD model with thermal activation, when the substrate temperature increases, the film becomes smooth and the void defect density decreases while the roughness increases slower.

Department.......Physics... Student's signature ....Narong Chanlek....

Field of study....Physics.... Advisor's signature ....Patcha Chatraphorn....

Academic year...2005........ Co-advisor's signature Nakorn Phaisangittisakul

Acknowledgements

First, I would like to thank my advisor, Asst. Prof. Dr. Patcha Chatraphorn and my co-advisor Dr. Nakorn Phaisangittisakul very much for their guidance and suggestion during this work. I also wish to thank Dr. Sojiphong Chatraphorn for the facility on high efficiency computer for my work. I thank the staffs and the students of CMRG who have helped me in various ways, especially, my colleagues Piti Panichayunon, Rachan Rangdee, Suwakan Piankoranee and Soontorn Chanyawadee.

I am also grateful to Assoc. Prof. Dr. Prapaipan Chantikul, Asst. Prof. Dr. Udomsilp Pinsook and Dr. Nuttakorn Thubthong for serving as a chairman and the committee respectively. All of whom have made valuable comments and have been helpful in the production of this thesis.

This thesis was supported financially by the Development and Promotion of Science and Technology Talents Project (DPST).

Finally, a deep affectionate gratitude is acknowledged to my family for love, understanding, and encouragements throughout the entire study.

สถาบันวิทยบริการ
จุฬาลงกรณ์มหาวิทยาลัย

Table of Contents

Abstract (Thai) .... **iv**

Abstract (English) .... **v**

Acknowledgements .... **vi**

Table of Contents .... **v**

List of Tables .... **ix**

List of Figures .... **x**

Chapter

I Introduction **1**

II Molecular Beam Epitaxy Growth and Models **3**

2.1 Molecular Beam Epitaxy Growth 3

2.1.1 Deposition 4

2.1.2 Desorption 5

2.1.3 Surface Diffusion 5

2.2 Models 5

2.2.1 Random Deposition (RD) Model 6

2.2.2 Random Deposition (RD) Model with Thermal Activation 6

2.2.3 Ballistic Deposition (BD) Model 9

2.2.4 Ballistic Deposition (BD) Model with Thermal Activation 10

สถาบันวิทยบริการ
จุฬาลงกรณ์มหาวิทยาลัย

III Methodology **12**

3.1 Working Procedure 12

3.2 Simulation Method 13

3.3 Quantities of Interest 15

3.3.1 Morphology 15

3.3.2 Defect Density 15

3.3.3 Interface Width 16

3.3.4 Height-Difference Correlation Function 17

3.4 Simulator Implementation 17

IV Results and Discussions **18**

4.1 Random Deposition (RD) Model 18

4.2 Random Deposition (RD) Model with Thermal Activation 23

4.3 Ballistic Deposition (BD) Model 36

4.4 Ballistic Deposition (BD) Model with Thermal Activation 42

4.5 Discussions 53

V Conclusions **59**

References **62**

Vitae **65**

สถาบันวิทยบริการ
จุฬาลงกรณ์มหาวิทยาลัย

List of Tables

3.1 The Arrhenius hopping rate and hopping time at various substrate temperatures. 15

สถาบันวิทยบริการ
จุฬาลงกรณ์มหาวิทยาลัย

List of Figures

2.1 The basic MBE growth process 4

2.2 The schematic representation of the RD model 8

2.3 The schematic representation of the RD model with thermal activation 8

2.4 The schematic representation of the BD model 11

2.5 The schematic representation of the BD model with thermal activation 11

4.1 Plot of the height $h(x)$ versus x of the RD model on the substrate size $L = 500$ at 50 MLs 19

4.2 The simulated schematic diagram of the RD model for the substrate size $L = 500$ at $t = 50$ MLs 19

4.3 Plot of the defect density $D(t)$ versus the log time t in the RD model for the substrate size $L = 500$ 20

4.4 Plot of the height $h(x)$ versus x of the RD model on the substrate size $L = 500$ at $t = 50$, 250 and 500 MLs 21

4.5 Plot of the interface width $W(t)$ versus the time t of the RD model for the substrate size $L = 500$ 22

4.6 Plot of the height-difference correlation function $G(r)$ versus r for various t in the RD model for the substrate size $L = 500$ 22

4.7 Plot of the height-difference correlation function $G(r)$ versus t at $r = 250$ in the RD model for the substrate size $L = 500$ 23

4.8 Plot of the height fluctuation versus x of the RD model with thermal activation at $T = 400$, 450, 500, 550, 600, 650 and 700 K for $t = 500$ MLs on the substrate size $L = 500$ 25

4.9 The simulated schematic diagram of the RD model with thermal activation for $T = 400$ K and the substrate size $L = 500$ at $t = 50$ MLs 26

4.10 The simulated schematic diagram of the RD model with thermal activation for $T = 500$ K and the substrate size $L = 500$ at $t = 50$ MLs 26

4.11 The simulated schematic diagram of the RD model with thermal activation for $T = 550$ K and the substrate size $L = 500$ at $t = 50$ MLs 27

4.12 The simulated schematic diagram of the RD model with thermal activation for $T = 600$ K and the substrate size $L = 500$ at $t = 50$ MLs 27

4.13 The simulated schematic diagram of the RD model with thermal activation for $T = 650$ K and the substrate size $L = 500$ at $t = 50$ MLs 28

4.14 The simulated schematic diagram of the RD model with thermal activation for $T = 700$ K and the substrate size $L = 500$ at $t = 50$ MLs 28

4.15 Plot of the defect density $D(t)$ versus the log time t in the RD model with thermal activation model for various T on the substrate size $L = 500$ 29

4.16 Plot of the defect density $D(t)$ versus the substrate temperature T in the RD model with thermal activation model on the substrate size $L = 500$ at $t = 50$ MLs 30

4.17 Plot of the interface width $W(t)$ versus the time t of the RD model with thermal activation for the substrate size $L = 500$ at $T = 400$, 450, 500, 550, 600, 650 and 700 K 32

4.18 Plot of the growth exponent β at the early time and the late time versus the substrate temperature T for the RD model with thermal activation 33

4.19 Plot of the height-difference correlation function $G(r)$ versus r for various t in the RD model with thermal activation at $T = 400$ K for the substrate size $L = 500$ 34

4.20 Plot of the height-difference correlation function $G(r)$ versus r for various t in the RD model with thermal activation at $T = 550$ K for the substrate size $L = 500$ 34

4.21 Plot of the height-difference correlation function $G(r)$ versus r for various t in the RD model with thermal activation at $T = 700$ K for the substrate size $L = 500$ 35

4.22 Plot of the height-difference correlation function $G(r)$ versus t at $r = 250$ and $T = 400$, 550, and 700 K in the RD model for the substrate size $L = 500$ 35

4.23 Plot of the height $h(x)$ versus x of the BD model on the substrate size $L = 500$ at 50 MLs and 500 MLs 37

4.24 Plot of the height $h(x)$ versus x of the BD model compares with the RD model at 500 MLs on the substrate size $L = 500$ 38

4.25 The simulated schematic diagram of the BD model at $t = 50$ MLs for the substrate size $L = 500$ 38

4.26 Plot of the defect density $D(t)$ versus the log time t in the BD model for the substrate size $L = 500$ 39

4.27 Plot of the interface width $W(t)$ versus the time t of the BD model for the substrate size $L = 500$ 40

4.28 Plot of the height-difference correlation function $G(r)$ versus r for various t in the BD model for the substrate size $L = 500$ 41

4.29 Plot of the height-difference correlation function $G(r)$ versus t at $r = 250$ in the BD model for the substrate size $L = 500$ 41

4.30 Plot of the height fluctuation versus x of the BD model with thermal activation at $T = 400$, 450, 500, 550, 600, 650 and 700 K for $t = 500$ MLs on the substrate size $L = 500$ 43

4.31 The simulated schematic diagram of the BD model with thermal activation for $T = 400$ K and the substrate size $L = 500$ at $t = 50$ MLs 45

4.32 The simulated schematic diagram of the BD model with thermal activation for $T = 500$ K and the substrate size $L = 500$ at $t = 50$ MLs 45

4.33 The simulated schematic diagram of the BD model with thermal activation for $T = 550$ K and the substrate size $L = 500$ at $t = 50$ MLs 46

4.34 The simulated schematic diagram of the BD model with thermal activation for $T = 600$ K and the substrate size $L = 500$ at $t = 50$ MLs 46

4.35 The simulated schematic diagram of the BD model with thermal activation for $T = 650$ K and the substrate size $L = 500$ at $t = 50$ MLs 47

4.36 The simulated schematic diagram of the BD model with thermal activation for $T = 700$ K and the substrate size $L = 500$ at $t = 50$ MLs 47

4.37 Plot of the defect density $D(t)$ versus the log time t in the BD model with thermal activation model for various T on the substrate size $L = 500$ 48

4.38 Plot of the defect density $D(t)$ versus the substrate temperature T in the BD model with thermal activation model on the substrate size $L = 500$ at $t = 50$ MLs 49

4.39 Plot of the interface width $W(t)$ versus the time t of the RD model with thermal activation for the substrate size $L = 500$ at $T = 400$, 450, 500, 550, 600, 650 and 700 K 50

4.40 Plot of the height-difference correlation function $G(r)$ versus r for various t in the BD model with thermal activation at $T = 400$ K for the substrate size $L = 500$ 51

4.41 Plot of the height-difference correlation function $G(r)$ versus r for various t in the BD model with thermal activation at $T = 550$ K for the substrate size $L = 500$ 51

4.42 Plot of the height-difference correlation function $G(r)$ versus r for various t in the BD model with thermal activation at $T = 700$ K for the substrate size $L = 500$ 52

4.43 Plot of the height-difference correlation function $G(r)$ versus t at $r = 250$ and $T = 400$, 550, and 700 K in the BD model for the substrate size $L = 500$ 52

4.44 Plot of the height fluctuation versus x of the BD model with thermal activation compares with the RD model with thermal activation for the substrate size $L = 500$ with the thickness 50 MLs at the substrate temperature $T = 500$ K and $T = 700$ K 54

4.45 Plot of the defect density $D(t)$ versus the substrate temperature of the BD model with thermal activation model compares with the RD model with thermal activation on the substrate size $L = 500$ at $t = 50$ MLs 55

4.46 Plot of the interface width $W(t)$ versus the growth time t on log-log scale of the BD model with thermal activation model compares with the RD model with thermal activation on the substrate size $L = 500$ at $T = 400$ K and 700 K 56

4.47 Bright field, cross-section TEM micrograph of a Si (100) homoepitaxial layer grown at $T = 548$ K 58

CHAPTER I

INTRODUCTION

Molecular beam epitaxy (MBE) is a standard technique to fabricate an epitaxy thin film [1, 2, 3]. This technique is of high interest because of its abilities to produce the high-quality thin film for a variety of materials. There are wide studies both theoretically and experimentally to understand the mechanism in the MBE growth. Several discrete models (e.g. Molecular Beam Epitaxy (MBE) model [2, 4, 5] and Wolf-Villain (WV) model [2, 6]) are studied in the literature. Most of these discrete models obey a condition that lattice defects such as vacancies and dislocations cannot occur in the film. This condition is known as the Solid-On-Solid (SOS) condition. However the defects can be found in the film during the experimentally MBE growth. These defects directly affect many important electronic and optical properties of the film so it is important to understand its behavior in the growth.

In this work, we propose two discrete models to simulate the void defect situation in the film. Our discrete models allow overhangs and bulk vacancies in the film to make them more realistic. They are called Random Deposition (RD) model with thermal activation and Ballistic Deposition (BD) model with thermal activation. In the RD model with thermal activation, the deposition rule is based on the Random Deposition (RD) model which is the simplest growth model. The model is defined with the SOS condition, which means bulk vacancy and overhanging of an atom are not permitted. In the BD model with thermal activation, the deposition rule is based on the Ballistic Deposition (BD) model. With the BD deposition rule, vacancies and overhanging are allowed to be created which is the main difference from the RD model. Our models treat the diffusion process, which is an essential process of the MBE, as a thermally activated Arrhenius hop-

ping process. The hopping rate is estimated using the Arrhenius expression which depends on the temperature of the substrate. The SOS condition is not used in this process. From our studies, we found that the substrate temperature has a strong effect on the properties of the film such as morphology, defect density and interface width.

In the next chapter, Chapter 2, we introduce the MBE growth and its essential mechanisms. The basic model, the RD model and the BD model, and our discrete models, the Random Deposition (RD) model with thermal activation and the Ballistic Deposition (BD) model with thermal activation, are explained. In Chapter 3, the simulation method and parameters which are used in the models are explained. We also introduce morphology, defect density, interface width and height-difference correlation function of the film in the last section. These interesting quantities are used to observe the growth and the quality of the film. In Chapter 4, our simulation results and discussions are presented. Finally, our conclusions are offered in Chapter 5.

CHAPTER II

MOLECULAR BEAM EPITAXY GROWTH AND MODELS

Epitaxy or epitaxial growth is a growth of thin film layer of one material on a crystal substrate. The crystalline of both materials have the same crystal structure. The film can be the same material as the substrate, in which case it is called *homoepitaxial* growth. Alternatively, the growth is called *heteroepitaxial* growth if the film is a different material from the substrate. In the first section, Molecular Beam Epitaxy (MBE) which is a technique of the epitaxial growth, and its basic processes are introduced. In the last section, we propose and explain discrete models applying to simulate the MBE.

2.1 Molecular Beam Epitaxy Growth

Molecular beam epitaxy (MBE) is a standard technique to fabricate the epitaxial thin film [1, 2, 3]. This technique is of high interest and plays a major role in semiconductor technology because of its abilities to produce the high-quality thin film for a variety of materials with good control of the film thickness, doping concentration, and alloy composition.

In MBE growth, a beam of neutral atoms or molecules is generated from a material source, called effusion cell, and deposit on a flat substrate crystal which is held at a constant temperature in the range between $500 - 1000$ K, depending on the specific type of materials. Deposited atoms or molecules (called adatom) adopt the orientation of the substrate and incorporate with the film. All processes are

operated under ultra high vacuum (UHV) system (i.e., pressure lower than 10^{-10} torr) to decrease impurities. The film is grown with a slow growth rate on the order of a few angstrom per second. The deposited atom diffuses around to fill any gap on the surface to form complete layer at time which is called layer-by layer growth (i.e. the deposited atoms arrange complete layer before the new layer growth begins to form). The film from this growth has nearly no bulk defects and a smooth surface.

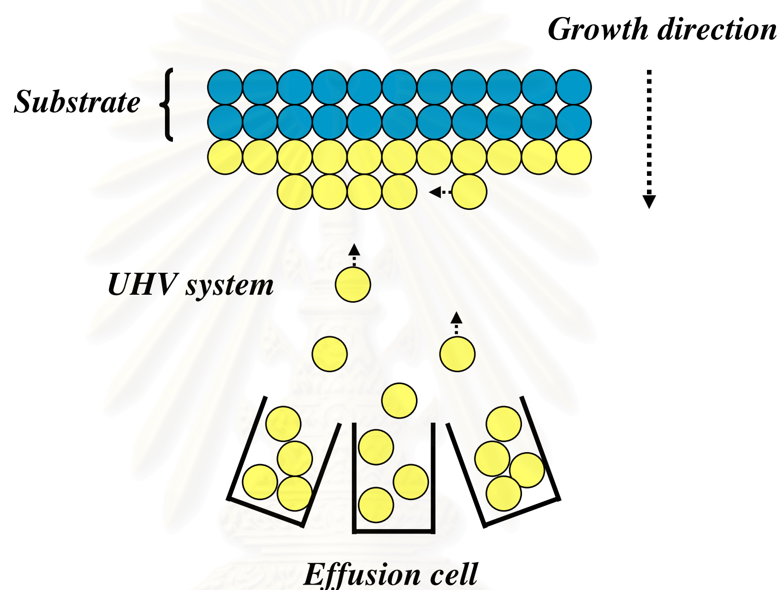

Figure 2.1: The basic MBE growth process.

There are three microscopic processes in the MBE growth which have important effects on the properties of the grown film. These processes are deposition, desorption and surface diffusion.

2.1.1 Deposition

Deposition is a process in which an atom randomly arrives on the surface of the substrate and forms the chemical bonds with its neighbors on the film. Rate of the deposition can be defined as a number of average completed layers of the thin film per unit time (ML/s). Typically, the MBE has small growth rate on order

of $0.1 - 1.0$ ML/s. The deposition rate is an important factor which affects the properties of the film.

2.1.2 Desorption

After an atom is deposited on the film, its chemical bonds can be broken and the atom leaves the surface of the film. This process which competes with the deposition process is desorption or reevaporation. The probability of the desorption depends on two parameters: energy of the deposited atom and strength of the bonds between the surface and the deposited atom . Typically, the desorption is rather small and can be neglected in some growth situations (e.g., Si, GaAs, etc.) [7].

2.1.3 Surface Diffusion

Generally, the deposited atom can move or diffuse on the surface of the film to search for an energetically most favorable position after the deposited atom sticks on the surface. This process is called surface diffusion which helps the atom to fill any gap on the surface and grow in layer-by-layer mode. In the MBE, the distance which an atom can diffuse from its deposited site depends on the substrate temperature and the binding energy.

2.2 Models

Modelling of the growth with a discrete model is a helpful tool to study the MBE growth. The model study can represent an essential link between the theory and experiment [8, 9]. There are many discrete models which can be applied to study the MBE, such as Das Sarma-Tamborenea (DT) model [2, 4, 10], Molecular Beam Epitaxy (MBE) model [2, 4, 5] and Wolf-Villain (WV) model [2, 6].

In this thesis, we propose two discrete models to study the homoepitaxial growth of the MBE which void defects can be formed. These models are based on the Random Deposition (RD) model [8, 11] and the Ballistic Deposition (BD)

model [2, 8, 12]. Our models and simulations are in $d'+d$ dimensional system where the atoms are deposited on a d' dimensional substrate leading to a d dimensional lattice crystal. In this thesis, we focus on $1+1$ dimensional system. An atom is represented by a unit-volume cube which can occupy only a discrete position on the lattice. All atomic coordinates are integral multiples of lattice spacing which are the same in horizontal and vertical direction. There are no off-lattice in our models. Size of the substrate (L) is defined to be a number of integral square lattice.

2.2.1 Random Deposition (RD) Model

Random deposition model is the simplest growth model. This model represents very low temperature MBE growth in which the atom deposits randomly and forms the chemical bond when it reaches the surface. The atom cannot move after deposits because it has low energy to break the bonds which it forms with the neighbors.

In this model, an atom is dropped randomly over the substrate and sticks instantaneously on the top of the surface where it arrives (see atom A and B in Fig. 2.2.). The atom permanently incorporates with the surface after it sticks. Solid-On-Solid (SOS) condition [8] - bulk vacancy, overhanging of an atom and desorption are not permitted - is satisfied in the model. Each column of the film grows independently because there is no correlation between neighbor sites. The height ($h_{(i,t)}$) of the surface at the location i increases independently in this model.

2.2.2 Random Deposition (RD) Model with Thermal Activation

Random Deposition (RD) model with thermal activation is developed from the RD model that includes the effects of surface diffusion. In this model, the deposition rule is based on the Random Deposition (RD) model with the SOS condition. We neglect the desorption process from this model because it is usually very small under typical MBE conditions. The surface diffusion process is applied to mimic

the realistic situation in the MBE growth. In our diffusion process, each surface atom (not only the freshly deposited atom) can diffuse or hop continuously to an empty neighboring site at anytime (not only at the time of its deposition) until it is completely buried by the other atom. The SOS condition is not used in this process. The hopping rate is given by Arrhenius expression [2, 7]

$$R_n = R_0 \exp(-\frac{E_n}{k_B T}), \tag{2.1}$$

where R_0 is a characteristic vibrational frequency, E_n is the activation energy for an atom with n nearest neighbors, k_B is the Boltzmann constant and T is the substrate temperature. The activation energy is the energy required for an atom to break its bonds at that site and hop to a neighboring site. It is given given by $E = E_0 + nE_b$ where E_0 and E_b are a ground activation energy and a bonding energy per neighbor. From the Arrhenius expression, the hopping rate of the surface atom depends on the initial configuration of the atom and the substrate temperature which effects the energy of atom.

Figure 2.3 is a diagram that illustrates the RD model with thermal activation. The yellow atom A, B, C and D show landing sites of the deposited atoms. These atoms cannot overhang due to the deposition rule of the RD model. When the surface atom is selected to hop, it chooses the site to which it will hop randomly from the eight sites forming a box around it. This landing site must provide at least one nearest neighbor bond (the dot squares show the possible hopping sites). For example, atom A can move to the left or right next-nearest neighbor site. Atom B can move to the left site or move down to the diagonally adjacent next-nearest neighbor site. The SOS condition is not used in this process so the atom can move up or down the cliff and overhang. As illustrated by atom C and D, atom C can move to the left site or move up the cliff to the next-nearest neighbor site and overhangs. Atom D can move up or move down to diagonally adjacent next-nearest neighbor site and overhangs. In this case, void can be formed in the film.

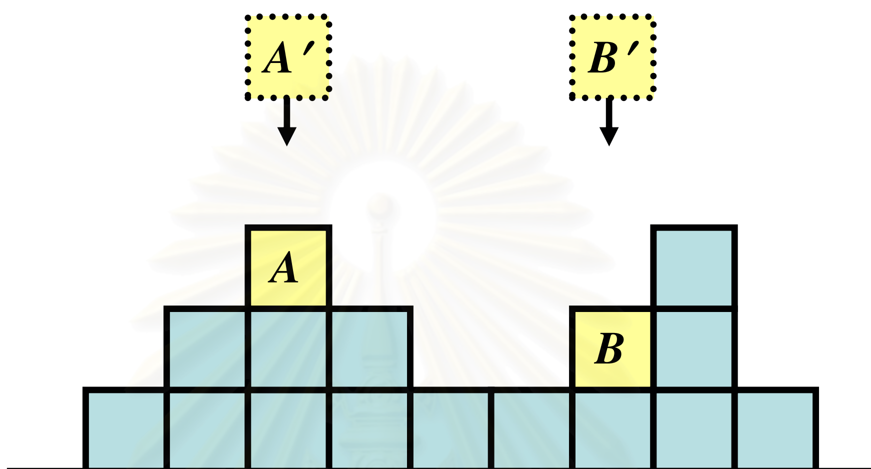

Figure 2.2: The schematic representation of the RD model.

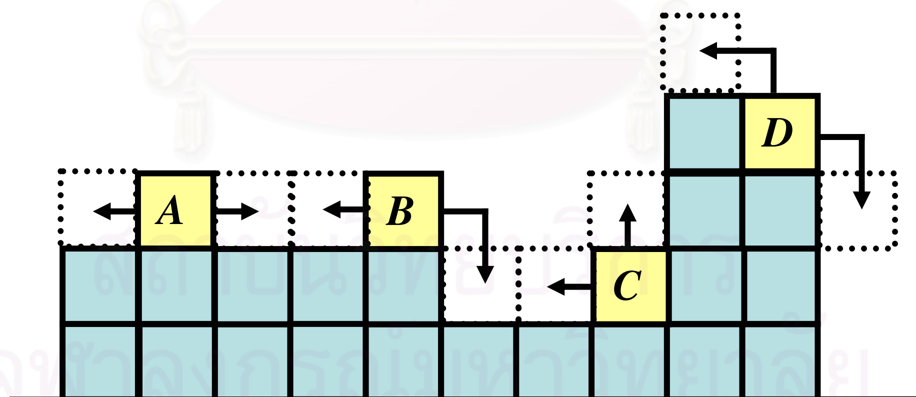

Figure 2.3: The schematic representation of the RD model with thermal activation.

From the rule of our model, the void defect cannot be formed in the deposition process due to the SOS condition. After the surface diffusion process, the void defect can be formed in the film because the surface atom can diffuse randomly without the SOS condition.

2.2.3 Ballistic Deposition (BD) Model

Ballistic deposition model was first proposed by Vold and Suntherland [12] as a model of colloidal aggregation. After that, the interest in this model has shifted toward the study of the film growth. This model represents very low temperature MBE growth in which the atom deposits randomly and forms the chemical bond at a first point of contact with the growing aggregate. This deposition rule can be considered as the low-energy deposited atom which is easily captured because of its low kinetic energy. The atom cannot move after deposits because it has low energy to break the bonds which it forms with the neighbors.

In this model, an atom is dropped randomly over an initially flat substrate. Figure 2.4 is a diagram that illustrates the BD model. The atom falls vertically (as atom A′ and B′ in Fig. 2.4) until it reaches the surface and sticks at a first point of contact with the growing aggregate. This means the atom sticks if it falls on top of the surface (atom A in Fig. 2.4.) or immediately next to the surface (atom B in Fig. 2.4.). From this rule, the height ($h(i,t)$) of the surface at the location i correlates with the height of nearest-neighbor sites as

$$h(i,t) \equiv max(h(i-1,t), h(i,t)+1, h(i+1,t)). \tag{2.2}$$

The SOS condition is not satisfied in this model. There are overhangs and void defects in the bulk which results in not densely film. Volume of the film in the BD model (V_{BD}) is not equal to the total volume of the deposited atoms (V_{tot}). To be explicit, in the BD model, $V_{BD} \geq V_{tot}$ for any growth time.

2.2.4 Ballistic Deposition (BD) Model with Thermal Activation

In this model, the deposition rule is based on the Ballistic Deposition (BD) model. The SOS condition is not satisfied in the deposition process. The surface diffusion process is then applied. The diffusion process of this model obeys the same diffusion rule as the Random Deposition (RD) model with thermal activation. The desorption process is still neglected in this model because it is usually very small under the typical MBE conditions. Physically, this deposition rule can be considered as the low-energy deposited atom which is easily captured because of its low kinetic energy.

Figure 2.5 is a diagram that illustrates the RD model with thermal activation. The yellow atom A, B, C and D show landing sites of the deposited atoms. In the deposition process, the deposited atoms can overhang, as illustrated by atom B and C. This is different from the RD model with thermal activation. In the diffusion process, the surface atom can move randomly to the landing site that provides at least one nearest neighbor bond (the dot squares show the possible hopping sites). This process is the same as in the Random Deposition (RD) model with thermal activation. The SOS condition is not used in this process. As illustrated in Fig. 2.5, atom A can move to the left or right next-nearest neighbor site. Atom B which overhangs can move up to the diagonally adjacent next-nearest neighbor site or move down the cliff which fills the gap on the film. Atom C can move up or down the cliff and overhangs. Atom D can move up the cliff and overhangs or move to the right next-nearest neighbor site and overhangs.

From our definition of the BD model with thermal activation, the void defect can be formed during both the deposition and the diffusion process. This is in contrast to the RD model with thermal activation where the void defects are created only during the diffusion process.

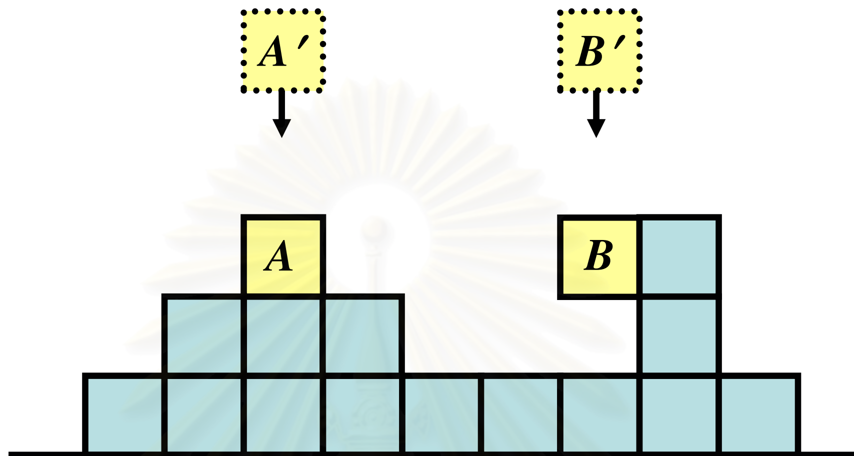

Figure 2.4: The schematic representation of the BD model.

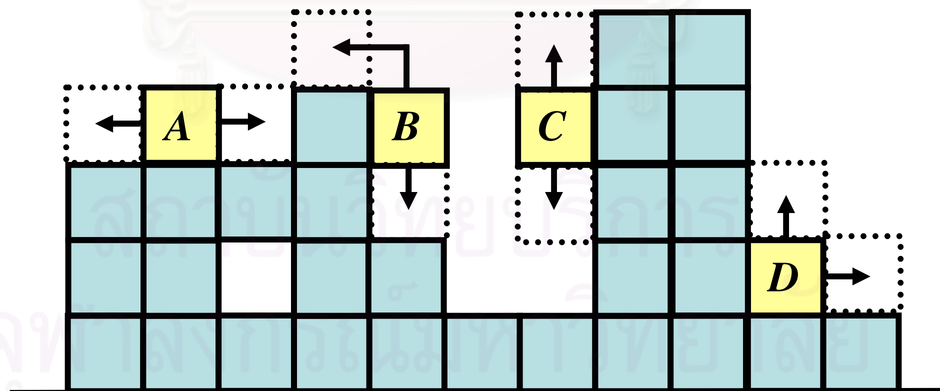

Figure 2.5: The schematic representation of the BD model with thermal activation.

CHAPTER III

METHODOLOGY

Computer simulation and modelling of thin film growth using a discrete model is a helpful tool to study the growth process. The simulation can be an essential link between theoretical works and experiments. In this chapter, we explain the simulation method and parameters which are used in the models. Interesting quantities used to characterize the simulated films are also introduced in this chapter.

3.1 Working Procedure

In this study, the working procedure can be summarized as follow:

1. The discrete model which is defined in the previous chapter is constructed using computer programming. Detail of the simulation method will be explained in the next section. The codes for the simulation were written on C language.

2. The parameters and growth conditions of the simulation is set up. In the simulation, we vary the substrate temperature of the growth in the range of 400 K to 700 K. Other details of the simulation parameter are shown in the next section.

3. The discrete model is simulated. Data of the simulated film, such as the position of the atom and the height of the film, is collected. The quantities of our interest which are used to characterize the film are calculated. These quantities will be introduced in the third section. The quantities of our

interest must be averaged in the calculation (except the morphology) so we make 20 runs to calculate the averaged values of these quantities. This step took several hours to many day depending on the growth conditions. For example, the running time for the BD model with thermal activation with substrate temperature $T = 550$ K, substrate size 500 and thickness 500 MLs is approximately 4 days for 20 runs.

4. Analyse the obtained data.

3.2 Simulation Method

In our simulation, all growth times are given in units of one completed layer (monolayer, ML) deposition, which is equivalent to the deposition of L atoms onto a substrate of size L. There are two main processes: deposition of adatoms and diffusion of surface atoms. In the deposition process, an atom is dropped randomly over the substrate which starts out flat. Here, the deposition rate is fixed at 1 ML/s (an average of one complete layer in one second). To be specific, this means within 1 second of growth time, a total of L atoms are deposited onto the substrate when L is the number of lattice sites on the substrate. A period of time an atom takes during its deposition process is the inverse of the deposition rate. So a deposition time of a single atom is $1/L$ second. In the simulation, positions of all atoms are kept and updated continuously during the growth. In the diffusion process, a list of the surface atoms eligible to diffuse (atom with n = 1, 2, 3) are kept and updated during the growth. When the diffusion process is activated, a surface atom with the highest probability to hop is selected. If there are more than one atom with the same highest probability to hop, only one atom will be randomly selected and allowed to diffuse. This atom will diffuse following the diffusion rule of the model. The probability to hop of each atom is the hopping rate R_n given by the Arrhenius expression Eq. (2.1). A period of time which an atom with n nearest neighbors needs in order to complete a hop to a neighboring site is called the hopping period τ_n. It is the inverse of the hopping rate ($\tau_n = 1/R_n$). The computer simulation algorithm can be summarized as follow:

1. Choose a dropped site x randomly and deposited an atom at that site by increasing the $h(x,t)$ at that site following the deposition rule.

2. Update and keep the position of the atom.

3. List the surface atoms eligible to diffuse.

4. Select one atom to diffuse. If there are more than one atom with the same highest probability to hop, only one atom will be randomly selected.

5. The selected atom diffuses randomly to an empty site following the diffusion rule.

6. Calculate the hopping period of the surface atom with highest probability to diffuse and keep in a counter variable.

7. Compare counter variable of the hopping period with the deposition time. If the counter variable is still less than the deposition time, the algorithm in step 2-5 are repeated.

8. Repeat all algorithm until the total number of deposited atoms reaches the predetermined value.

In our simulation, the parameters in the Arrhenius expression are set to be $E_0 = 1.0\ eV$ and $E_b = 0.3\ eV$. We show the hopping rate and hopping time of the surface atom with $n = 1$ and $n = 2$ at various substrate temperature in Table 3.1. Periodic boundary condition is applied in our models to eliminate the effect of the edge and to reduce the finite size effect. To improve the effectiveness of the simulation, diffusion of a surface atom with $n > 2$ is forbidden. This is because an atom with $n > 2$ is bounded relatively tightly with its neighbors and requires too much energy to break away from the film.

Table 3.1: The Arrhenius hopping rate and hopping time at various substrate temperatures.

T (K)	$R_{n=1}$	$\tau_{n=1}(s)$	$R_{n=2}$	$\tau_{n=2}(s)$
400	3.4×10^{-4}	2.9×10^{3}	5.7×10^{-8}	1.8×10^{7}
450	2.6×10^{-2}	38.5	1.1×10^{-5}	9.1×10^{4}
500	0.8	1.2	7.7×10^{-4}	1.3×10^{3}
550	13.9	7.2×10^{-2}	2.5×10^{-2}	40
600	1.5×10^{2}	6.7×10^{-3}	0.5	2.2
650	1.12×10^{3}	8.9×10^{-4}	5.26	0.2
700	6.3×10^{3}	1.6×10^{-4}	43.6	2.3×10^{-2}

3.3 Quantities of Interest

3.3.1 Morphology

In high quality MBE growth, the grown film should be a smooth surface and has no void defect. This film has an good contact properties and is suitable for semiconductor device. The morphology is a common quantity which shows the general quality of the film. In this work, we use a plot of $h(x, t)$ as a function of x at fixed t and the schematic diagram which shows the position of the atoms in the film to show the morphology of the film. The height $(h(x, t))$ of the film is defined to be the value of the highest occupied site in column x at time t.

3.3.2 Defect Density

To observe the void formation in the film, we define defect density $D(t)$ which is a function of time t as

$$D(t) \equiv \frac{\textit{number of unoccupied sites in film}}{\textit{number of sites in film}} \equiv \frac{(V(t) - N)}{V(t)}. \qquad (3.1)$$

N is a number of deposited atom. V(t) is volume of the film. This quantity is, basically, a ratio of the void to the total volume of the film. It gives a quantitative answer to the question “ How many voids are there in the film ? ”

3.3.3 Interface Width

The interface width is a root mean square fluctuation of height ($h(x,t)$) of the surface. It is an effective tool to characterize the roughness of the film. The interface width, which is the function of the substrate size L and time t, is defined as [2, 8]

$$W(L,t) \equiv \left\langle (h(x,t) - \langle h(t) \rangle)^2 \right\rangle^{1/2}, \quad (3.2)$$

where $h(x,t)$ is the surface height at substrate site x and time t, $\langle h(t) \rangle$ is an average height at the time t which is calculated as in Eq. 3.3 , L is the size of the substrate, and $\langle ... \rangle$ means that the quantity in that bracket is averaged over the substrate, for example,

$$\langle h(t) \rangle \equiv \frac{1}{L} \sum_{x=1}^{N} h(x,t). \quad (3.3)$$

From the dynamical scaling hypothesis, the plot of $W(L,t)$ with time t can be divided into two regions. In the early time, the interface width increases as the power of time t [13, 14, 15] as

$$W(L,t) \sim t^{\beta} \ (small\ t). \quad (3.4)$$

The exponent β is the *growth exponent.* This constant can describe relation between the roughness of the growth and time. At large t, the interface width does not increase indefinitely, but it will saturate which depends on the substrate size L as

$$W_{sat}(L) \sim L^{\alpha} \ (large\ t). \quad (3.5)$$

The exponent α is the *roughness exponent.*

สถาบันวิทยบริการ
จุฬาลงกรณ์มหาวิทยาลัย

3.3.4 Height-Difference Correlation Function

Height-difference correlation function $G(r,t)$ is another way to characterize the roughness of the surface. This function is defined by a root mean square between two sites separated by the distance r,

$$G(r,t) = \left\langle |h(x+r,t) - h(x,t)|^2 \right\rangle^{1/2}, \tag{3.6}$$

where r is a distance between two sites on the substrate. This quantity provides a useful information in the surface height and the roughness of submonolayer regime. For varied r and fixed t, $G(r,t)$ can show how the surface height correlates to the neighboring sites. Alternately, for varied t and fixed r, $G(r,t)$ can show how the the roughness of submonolayer evolves with time.

3.4 Simulator Implementation

In this work, the simulator was written on C language using gcc-lib version 2.95.3 and operated on Linux using a re-compile kernel version 2.4.24 to accommodate symmetric multi-processing (SMP). For the computer facilities, we carry out the simulations on computers based on Intel Pentium 4 Hyper-threading running at 3.2 GHz with base-memory of 1 GB.

สถาบันวิทยบริการ
จุฬาลงกรณ์มหาวิทยาลัย

CHAPTER IV

RESULTS AND DISCUSSIONS

In this chapter, the simulation results from our discrete models are presented. All of the simulations are done in 1+1 dimensional system on the initially flat substrate. The deposition rate is fixed at one monolayer (ML) per second. First, we show the results of Random Deposition (RD) model and Random Deposition (RD) model with thermal activation. Next, the results of Ballistic Deposition (BD) model and Ballistic Deposition (BD) model with thermal activation are shown. Our films are studied through their morphologies, interface widths, defect densities and height-difference correlation functions which are defined in the previous chapter. Finally, our results are discussed.

4.1 Random Deposition (RD) Model

The RD model is the simplest growth model. In this model, an atom is dropped randomly over an initially flat substrate and then incorporated permanently into the film. The SOS condition is satisfied in this process. The surface diffusion and desorption process are neglected in this model.

To characterize a surface morphology of the RD model, the height $h(x)$ for the substrate site $L = 500$ and the growth time $t = 50$ MLs is plot as a function of column site x as shown in Fig. 4.1. It can be observed that the morphology is very rough. This result shows that the height of the film at each position on the substrate increases independently because a deposited atom is dropped randomly and cannot diffuse after it is deposited. The simulated schematic diagram which shows the position of the atoms in the film is shown in Fig. 4.2. It is obvious

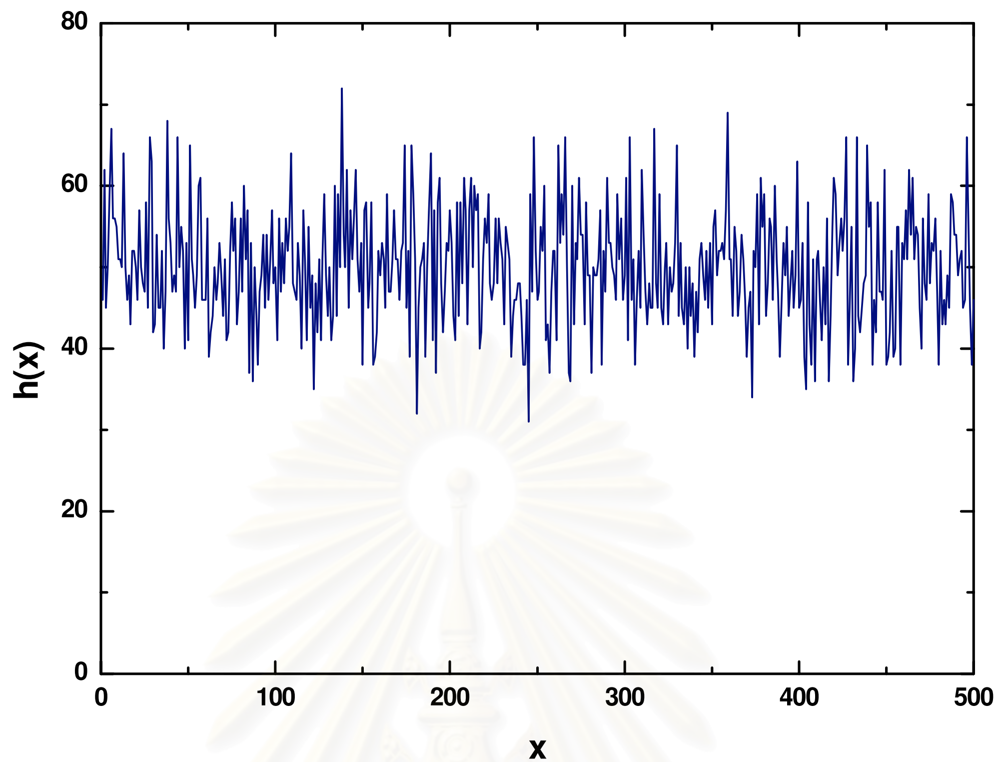

Figure 4.1: Plot of the height $h(x)$ versus x of the RD model on the substrate size $L = 500$ at 50 MLs.

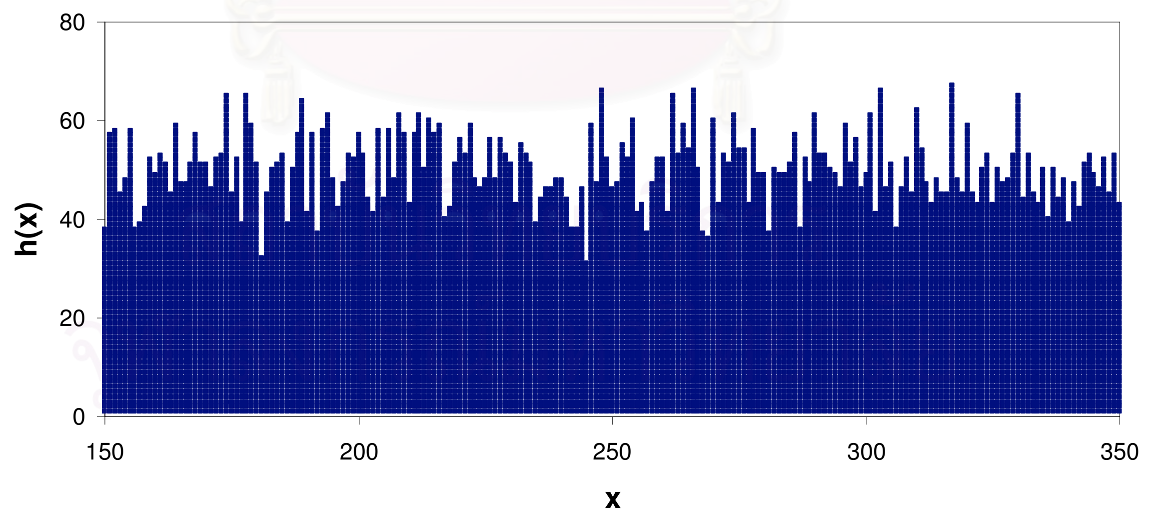

Figure 4.2: The simulated schematic diagram of the RD model for the substrate size $L = 500$ at $t = 50$ MLs expands view of $x = 150 - 350$.

that the film has a compact bulk. The void defect can not be formed. An average height of the film for growth time $t = 50$ MLs is 50 MLs. This result shows that a volume of the film of the RD model is conserved because the SOS condition is followed in this model. Under this condition, bulk vacancy, overhanging of an atom and desorption cannot be created. To make sure that the computer program is correct, and for comparison with results of the other models later, the defect density is calculated for the RD model. In Fig. 4.3, a plot of the defect density $D(t)$ with time t shows that $D(t)$ is zero for all growth time. This result confirms that the void defect cannot be created in the film.

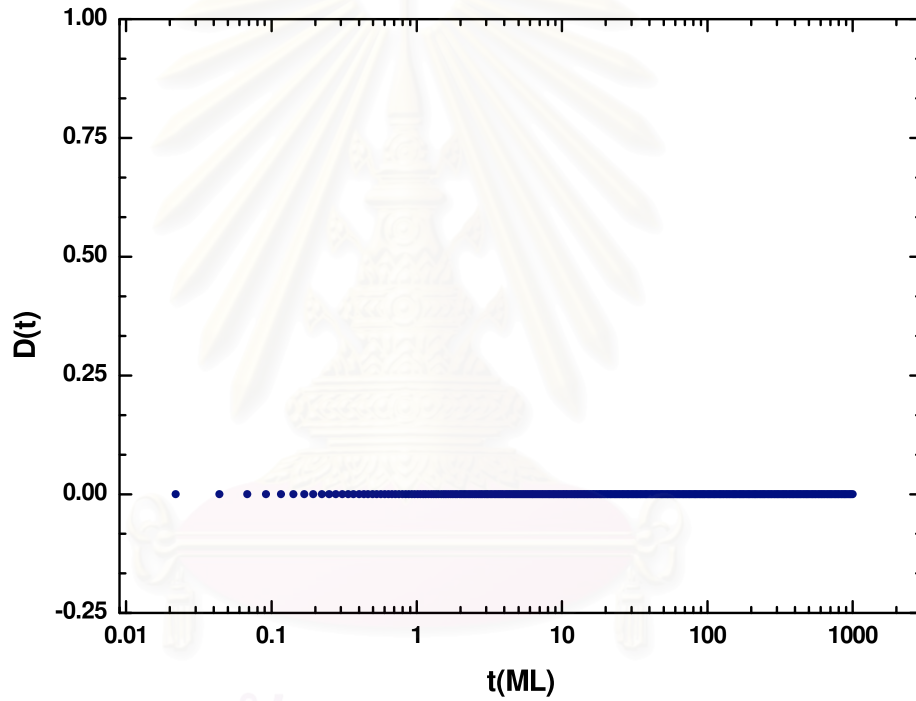

Figure 4.3: Plot of the defect density $D(t)$ versus the log time t in the RD model for the substrate size $L = 500$.

To characterize the roughness, we plot the height $h(x)$ as a function of column site x which shows the simulated surface morphology of the RD model for the growth time of 50, 250 and 500 MLs and the substrate size $L = 500$ as shown in Fig. 4.4. This figure shows that the film roughness increases as the time increases. To characterize the roughness, we plot the interface width $W(t)$ versus the time t on log-log scale as shown in Fig. 4.5. It is observed that the $W(t)$

increases as the power of t. The slope of this plot is the growth exponent β. The straight line in Fig. 4.5 indicates the best fit which yields the value of β. We found that β is approximately 0.5. A height-difference correlation function $G(r)$ which is plotted versus the distance r on log-log scale for time $t = 1$ to $t = 1000$ ML is shown as Fig. 4.6. From this plot, the height-difference correlation function do not depend on the distance between the two sites on the substrate. This result shows that the surface height increases independently without correlating to the neighboring sites. A plot of $G(r)$ versus t at $r = 250$ is show in Fig. 4.7. This results show that when the simulation time increases, the value of $G(r)$ tends to increase indefinitely. This result corresponds with the interface width that the roughness increases indefinitely with time. Our results agree with the others in the literature [8].

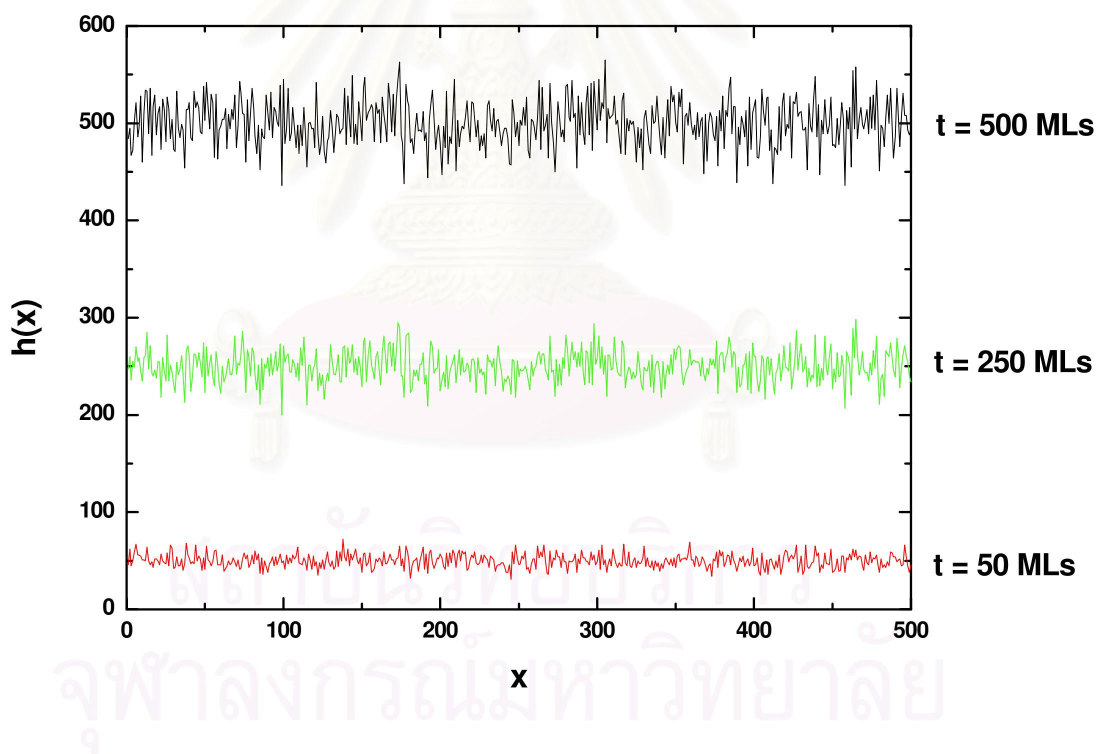

Figure 4.4: Plot of the height $h(x)$ versus x of the RD model on the substrate size $L = 500$ at $t = 50$, 250 and 500 MLs.

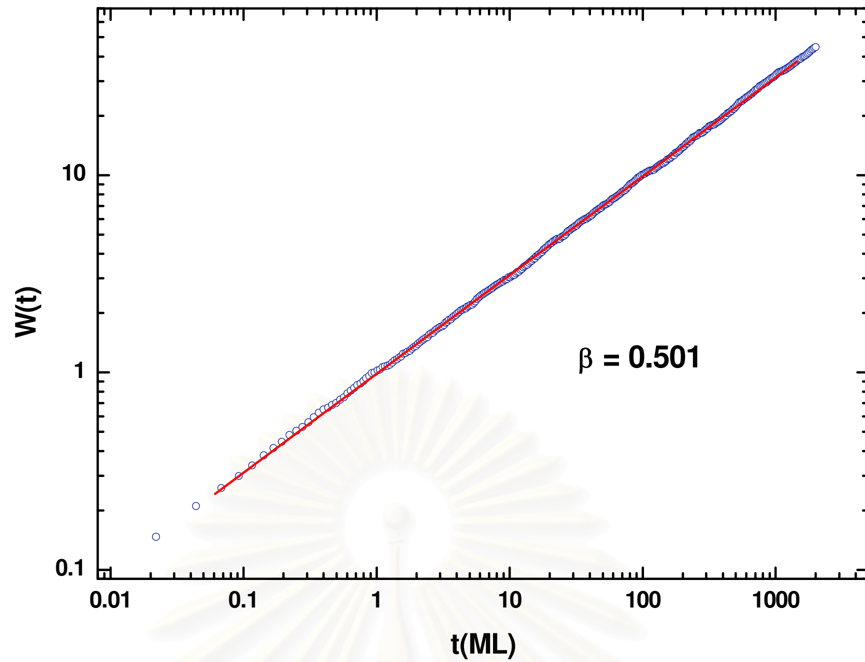

Figure 4.5: Plot of the interface width $W(t)$ versus the time t on a log-log scale of the RD model for the substrate size $L = 500$.

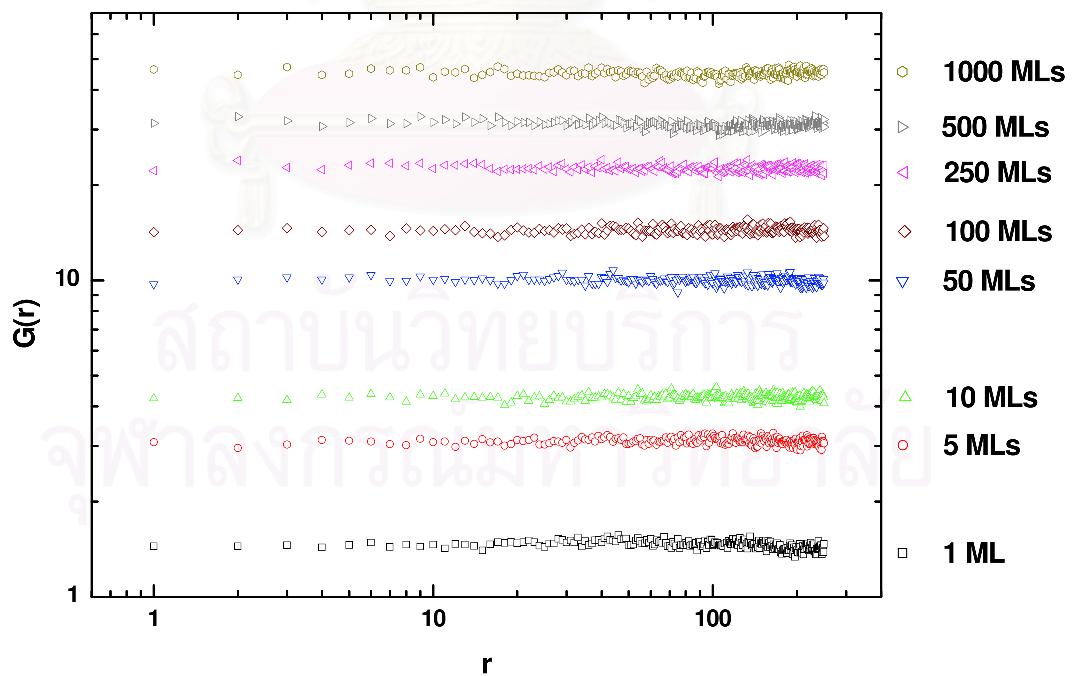

Figure 4.6: Plot of the height-difference correlation function $G(r)$ versus r on a log-log scale for various t in the RD model for the substrate size $L = 500$.

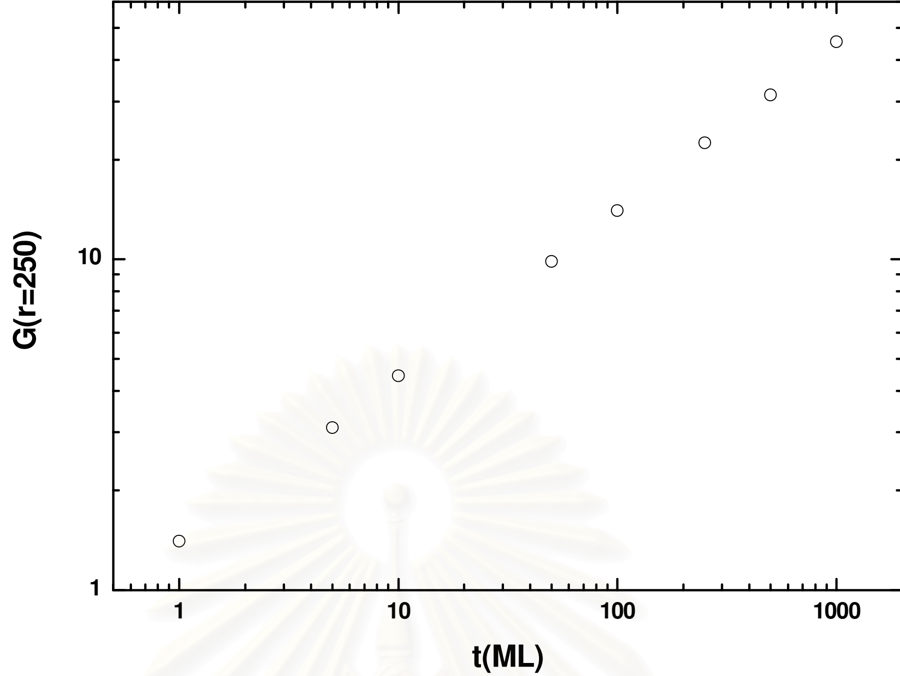

Figure 4.7: Plot of the height-difference correlation function $G(r)$ versus t on a log-log scale at $r = 250$ in the RD model for the substrate size $L = 500$.

4.2 Random Deposition (RD) Model with Thermal Activation

Random Deposition (RD) model with thermal activation is based on the RD model. We propose this model to study void defect formation and effects of the substrate temperature on the film. In this model, an atom is dropped randomly over an initially flat substrate following the deposition rule of the RD model. The SOS condition is satisfied in this process. The surface atom then can diffuse continuously to a random empty neighboring site. The SOS condition is not applied in the diffusion process so the void defect can be formed during diffusion. The hopping rate is calculated using the Arrhenius expression which depends on the temperature of the substrate and the configuration of the surface atom.

Fig 4.8 shows the plots of height fluctuation versus the column site x which show the surface morphologies of the films for the substrate site $L = 500$ and the thickness 50 MLs when the substrate temperature is varied from $T = 400$ K to

$T = 700$ K. The simulated schematic diagrams which show the position of the atoms in the film corresponding to these films are shown in Figs. 4.9 - 4.14. From the morphologies of the film, we can observe effects of the substrate temperature on the film. The surface of the films at low T $(400 - 500$ K) are very rough, similar to the surface of the RD model in Fig. 4.1. At higher temperature, however, the films become smoother. From Figs. 4.9 - 4.14, the number of void in the films seems to depend on the substrate temperature in a nontrivial way. The amount of unoccupied sites in the film starts from practically zero when $T = 400$ K, then increases when T increased, but then decreases to almost zero again when $T = 700$ K. To quantitatively study the void defect, we plot the defect density $D(t)$ versus the time t at the substrate temperature $T = 400$, 500, 550, 600, 650 and 700 K for $L = 500$ as shown in Fig. 4.15. The plot of the defect density at $t = 50$ MLS versus the substrate temperature is also shown in Fig. 4.16. It is observed that the defect density in each system increases with growth time. It was also found that the defect density depends on the substrate temperature. When the temperature is below 600 K, the void defect density increases with the substrate temperature. At higher temperatures, the void defect density decreases as the substrate temperature increases. This agrees with the morphologies shown in Figs. 4.9 - 4.14.

These results show that the substrate temperature has a strong effect on the morphology and the defect density of the grown film. From our results, we can divide the growth into two main regimes. In the first regime, the substrate temperature is low. The hopping rate is very low. The atom which is dropped randomly is deposited without any diffusion most of the time because the surface atom has low energy. Therefore the probability to diffuse is small. As a result, the films at low temperatures ($T < 500$ K) are very rough which is consistent to the RD model. When we increase the temperature, the surface atom increases the probability to diffuse. As a result, the void defects, which can be formed during the diffusion process, start forming and the void defect density increases with the substrate temperature in this regime. In the second regime, at high temperature, the hopping rate of the surface atom is high. The surface atom has high probability to diffuse to search for a suitable site that leads to layer-by-layer growth mode.

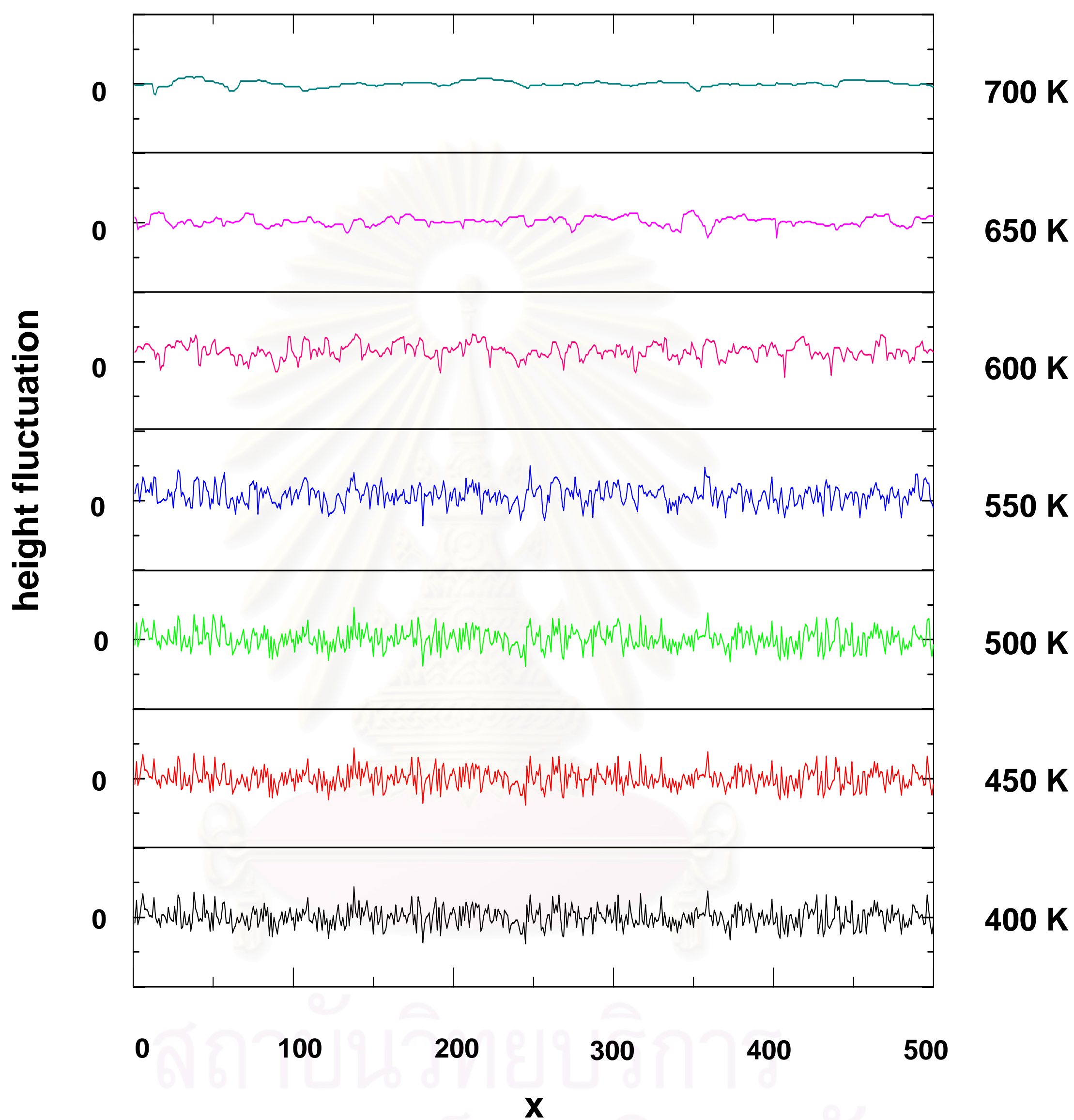

Figure 4.8: Plot of the height fluctuation versus x of the RD model with thermal activation at $T = 400$, 450, 500, 550, 600, 650, and 700 K for $t = 500$ MLs on the substrate size $L = 500$.

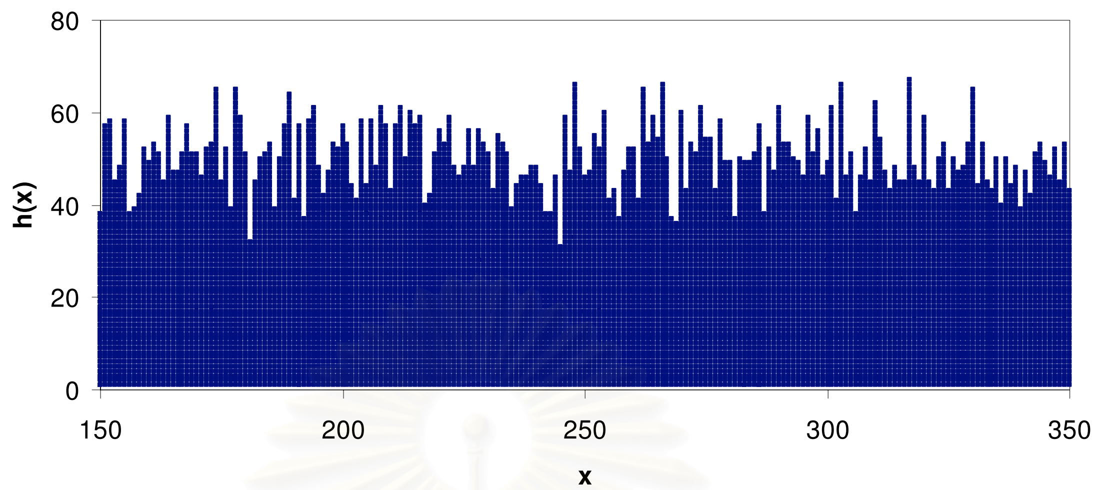

Figure 4.9: The simulated schematic diagram of the RD model with thermal activation for $T = 400$ K and the substrate size $L = 500$ at $t = 50$ MLs expands view of $x = 150 - 350$.

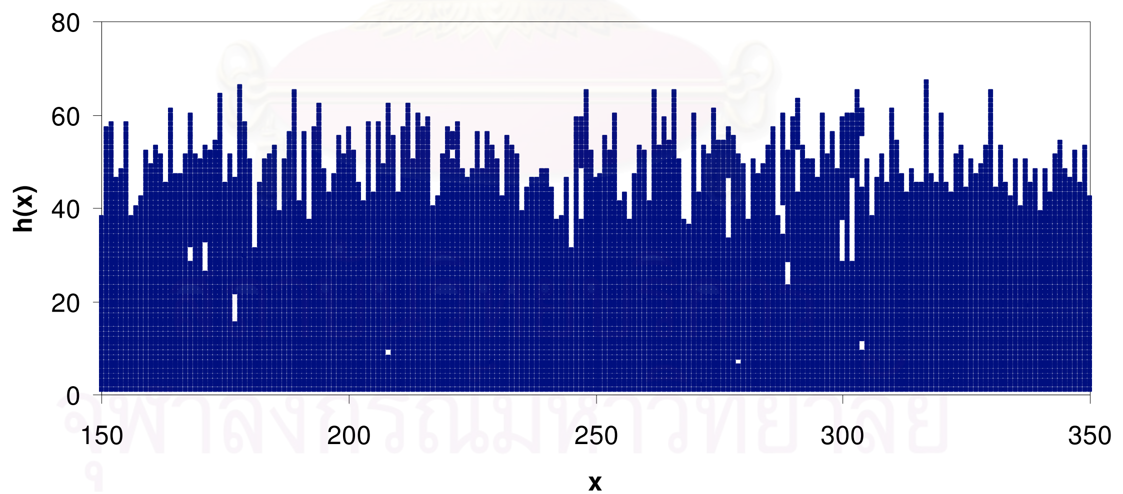

Figure 4.10: The simulated schematic diagram of the RD model with thermal activation for $T = 500$ K and the substrate size $L = 500$ at $t = 50$ MLs expands view of $x = 150 - 350$.

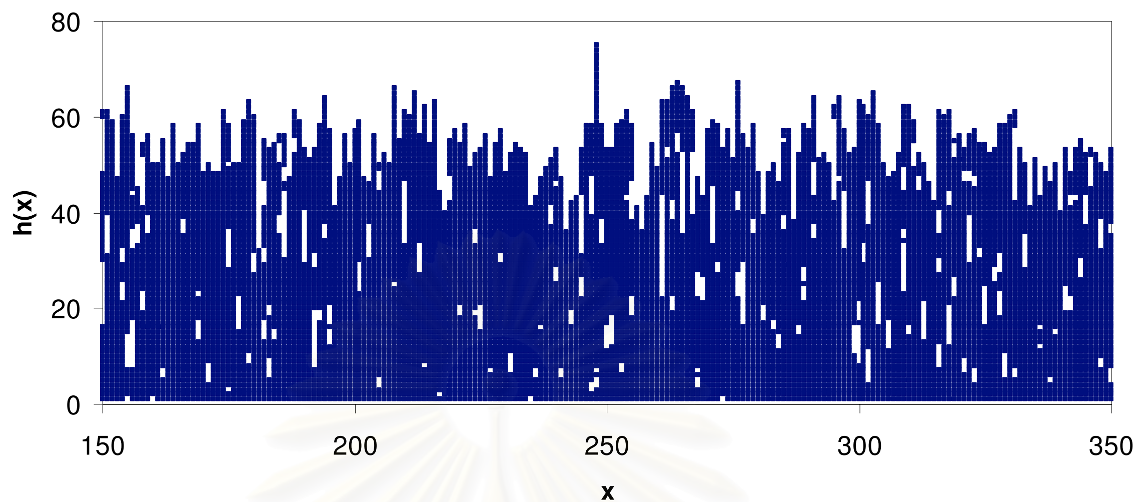

Figure 4.11: The simulated schematic diagram of the RD model with thermal activation for $T = 550$ K and the substrate size $L = 500$ at $t = 50$ MLs expands view of $x = 150 - 350$.

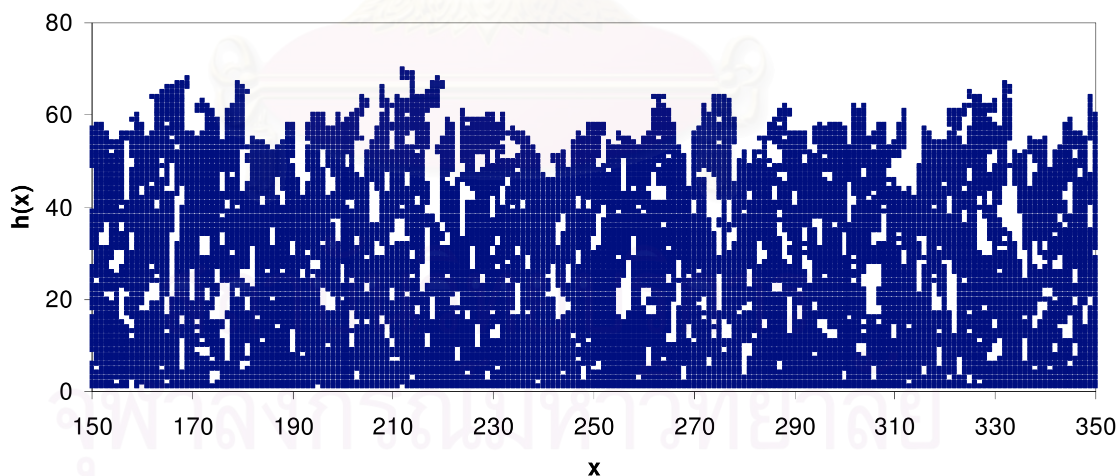

Figure 4.12: The simulated schematic diagram of the RD model with thermal activation for $T = 600$ K and the substrate size $L = 500$ at $t = 50$ MLs expands view of $x = 150 - 350$.

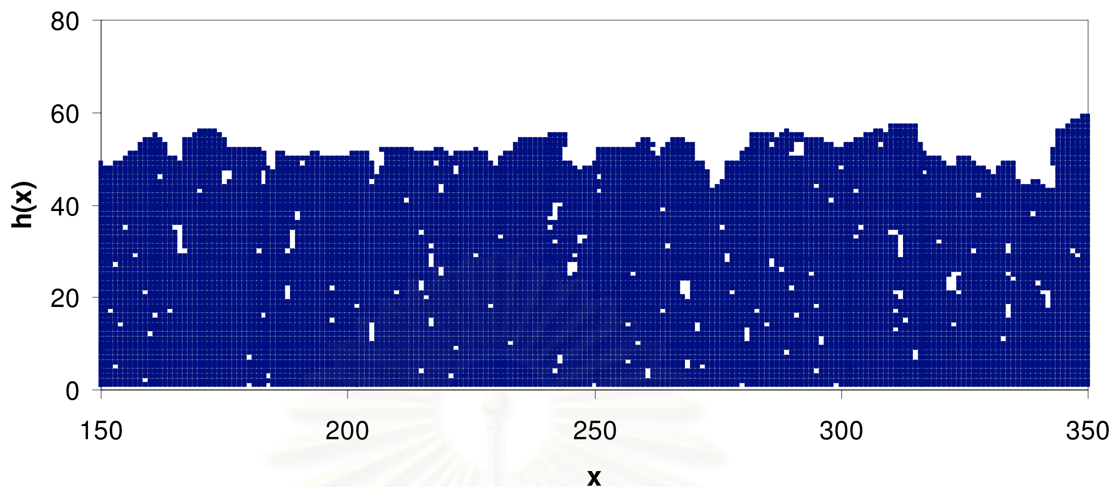

Figure 4.13: The simulated schematic diagram of the RD model with thermal activation for $T = 650$ K and the substrate size $L = 500$ at $t = 50$ MLs expands view of $x = 150 - 350$.

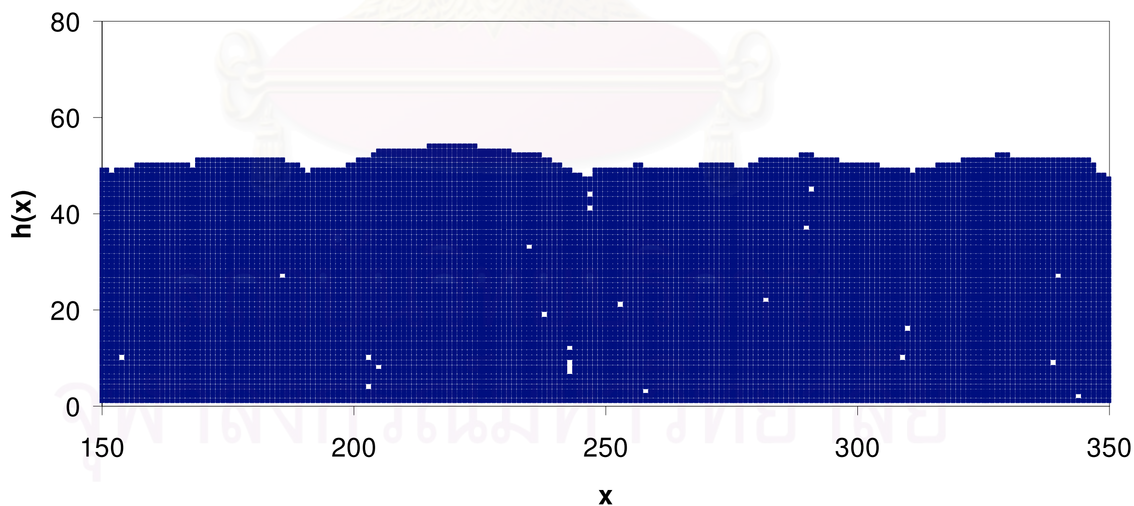

Figure 4.14: The simulated schematic diagram of the RD model with thermal activation for $T = 700$ K and the substrate size $L = 500$ at $t = 50$ MLs expands view of $x = 150 - 350$.

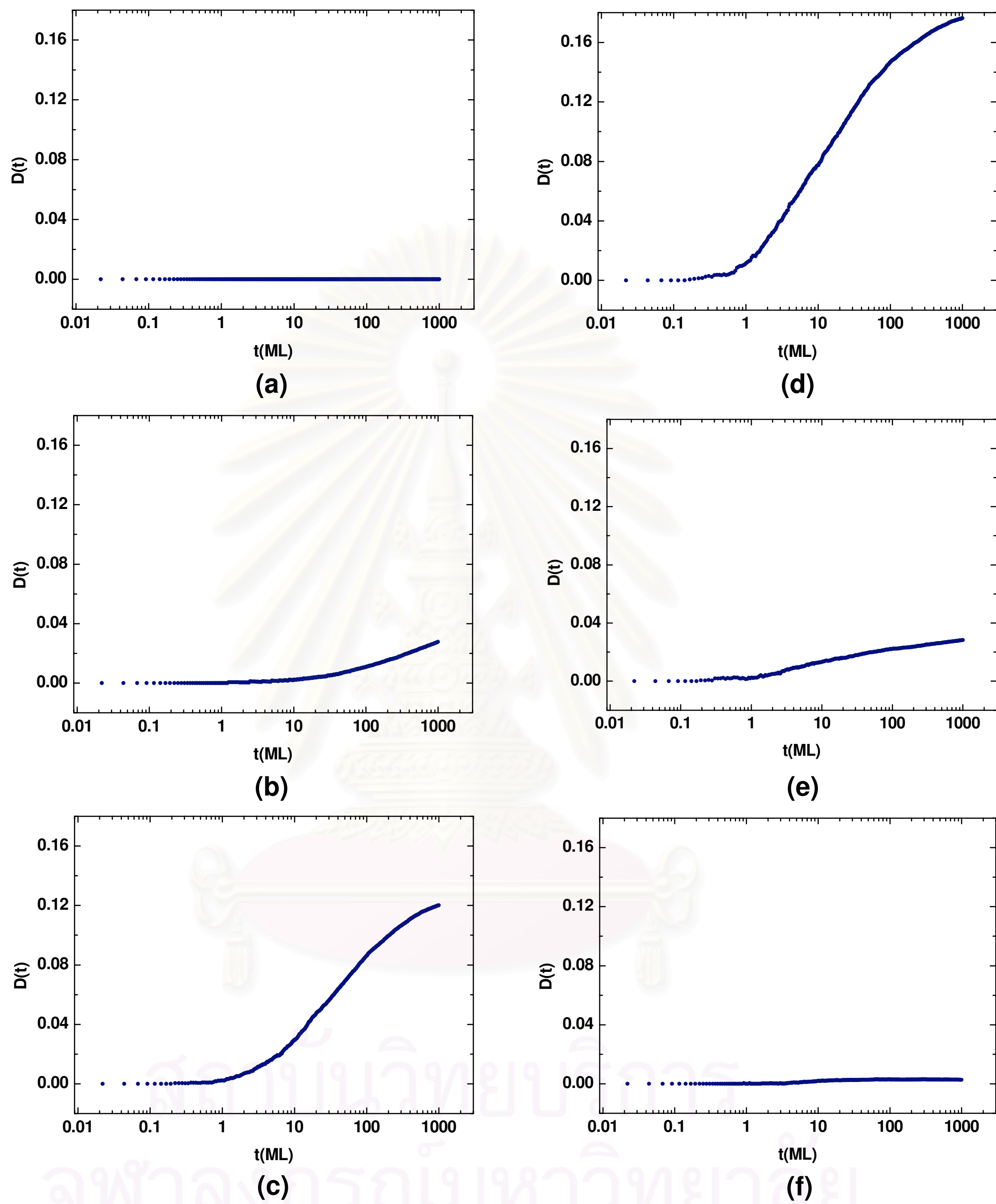

สถาบันวิทยบริการ
จุฬาลงกรณ์มหาวิทยาลัย

Figure 4.15: Plot of the defect density $D(t)$ versus the log time t in the RD model with thermal activation model for various T on the substrate size $L = 500$ (a) $T = 400$ K, (b) $T = 500$ K, (c) $T = 550$ K, (d) $T = 600$ K, (e) $T = 650$ K and (f) $T = 700$ K.

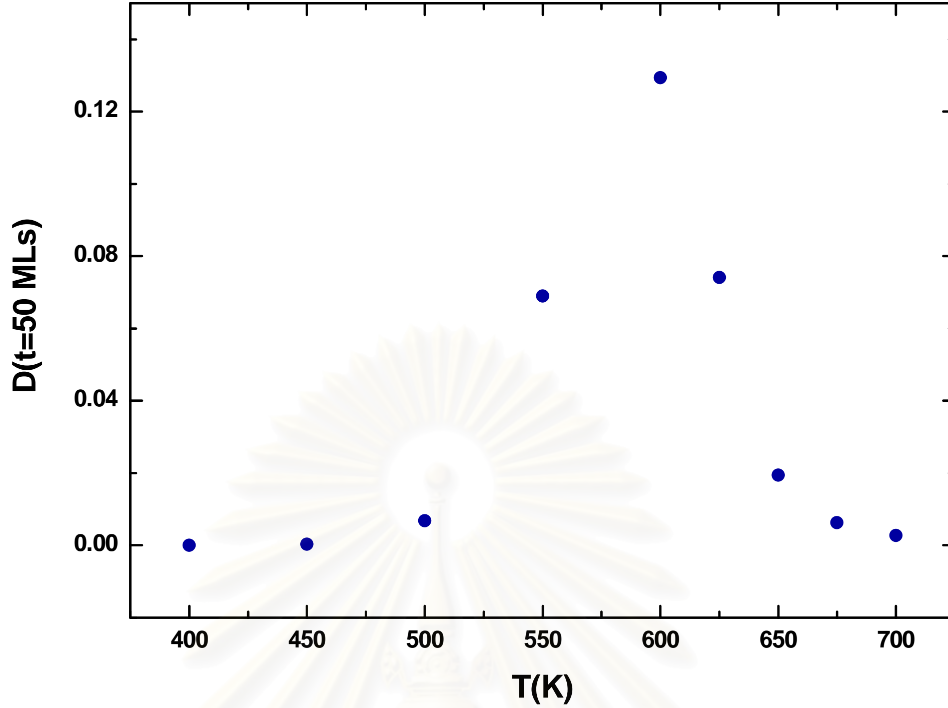

Figure 4.16: Plot of the defect density $D(t)$ versus the substrate temperature T in the RD model with thermal activation model on the substrate size $L = 500$ at $t = 50$ MLs.

As a result, the film becomes smooth and the void defect density decreases as the substrate temperature increases.

In Fig. 4.17, the interface width $W(t)$ of systems at the substrate temperature between $T = 400 - 700$ K are plotted as a function of the time t on log-log scale. It is obvious that the interface width of each system increases with the time. In very early time, i.e. before the first layer is complete ($t << 1$ ML), we found that the slope of these plots, which is the growth exponent β, are 0.5. This β is the same as in the RD model where the height of the film increases independently. This is because the substrate starts out as a flat surface. A number of incorporating atom is very small and the atoms widely spread over the flat substrate so the diffusion process has very small effect on the roughness of the film. As a result, $W(t)$ is similar to the RD model in the early time. For low temperature ($T < 550$ K), we found that $W(t)$ still have β at approximately 0.5 for the entire growth time. This is because the hopping rate is very low at low temperature. The surface

atom cannot diffuse much. As a result, $W(t)$ shows the same behavior as the RD model where there is no diffusion at all. At higher temperature ($T \geq 550$ K), the $W(t)$ shows a different behavior from the RD model. The slope of $W(t)$ is smaller than in the RD model. This result means that the roughness of the film grown at the high substrate temperature increases slower than the RD model film. We also found that the slope of $W(t)$ of various systems decreases when T increases at the early times ($t < 20$ MLs) and has the same value at the late time ($t > 50$ MLs). Figure 4.18 shows our measurements of β from $W(t)$ of Fig. 4.17, both at the early and the late time regimes. In the early time, the atom is deposited on the substrate which starts out as a flat surface. There are small fluctuations in the surface so a number of kink site, i.e. the site with more than one bond, is very small. From Arrhenius expression, if an atom sticks at a kink site, it will has very low probability to diffuse so it will remain there for a long time. The surface atom can diffuse long distance to search for a suitable site before it is trapped by the kink sites which are very rare in this regime. When we increase the temperature, the surface atom increases probability to diffuse. As a result, β decreases as T increases in the early time regime. In the late time, there are more fluctuations with large amplitude so a number of the kink site increases. When we increase the temperature, the surface has high probability to diffuse but it cannot diffuse long distance because it can be trapped easily by many kink sites on the film. Consequently, the slope of $W(t)$ has the same value in the late time regime. It is also found that the change of $D(t)$ in time corresponds with the change $W(t)$ in time. From Fig. 4.15, the temporal change in $D(t)$ of $T = 600$ at $t \sim 100$ MLs corresponds to the change in $W(t)$

In Figs. 4.19 - 4.21, we show the height-difference correlation function $G(r)$ versus the distance r at $t = 1$ to $t = 1000$ ML. We also show the plot of $G(r)$ versus t at $r = 250$ and the substrate temperature $T = 400$, 550, and 700 K on log-log scale is show in Fig. 4.43. At $T = 400$ K, $G(r)$ do not depend on r. The value of $G(r)$ increases indefinitely with t. This is because the hopping rate is very low. The atom is deposited randomly but has very low probability to move so $G(r)$ shows the behavior which is the same as in the RD model. At $T = 550$ K, $G(r)$ shows a different behavior from the RD model. For a small distance between

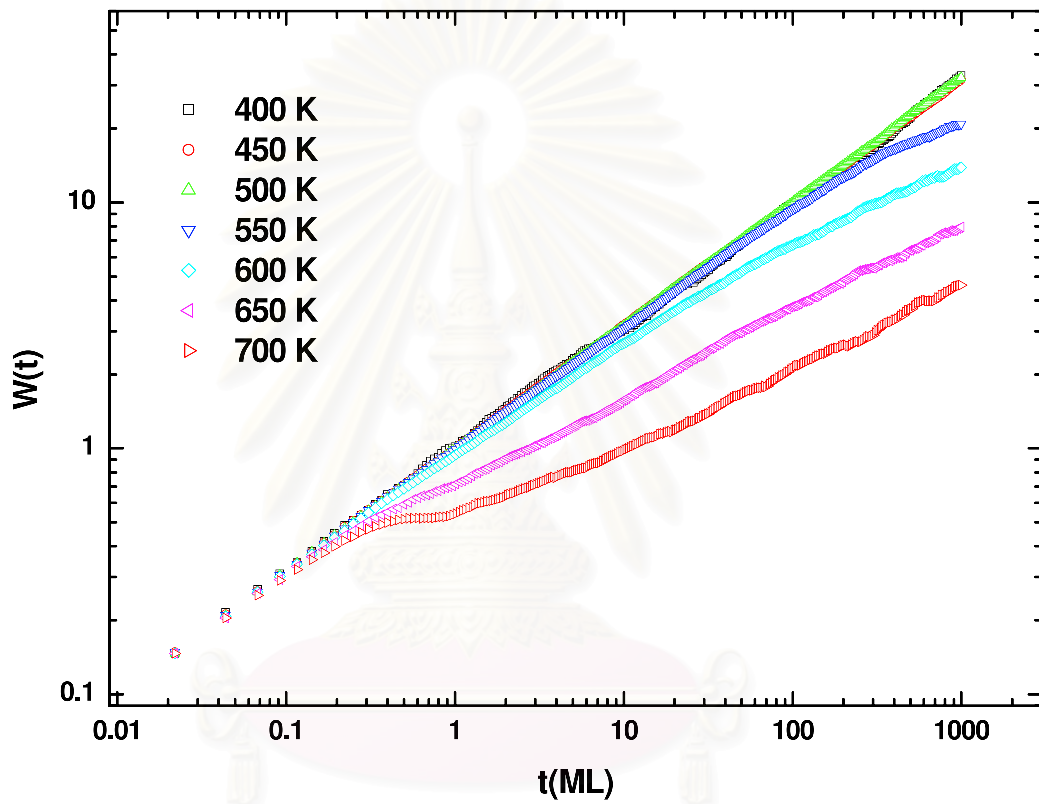

Figure 4.17: Plot of the interface width $W(t)$ versus the time t on a log-log scale of the RD model with thermal activation for the substrate size $L = 500$ at $T = 400$, 450, 500, 550, 600, 650 and 700 K.

two sites on the substrate, $G(r)$ tends to increase with r at the large time. At high temperature $T = 700$ K, the relation which $G(r)$ depends on r is dominant. The increment of $G(r)$ with t is slower. This result corresponds with the interface width that the roughness of the film increases slower when the temperature increases. This is because the surface atom can diffuse to a neighboring site. This process can decrease the difference of the neighboring sites. When T increases, the surface atom increases the probability to diffuse. As a result, $G(r)$ depends on a distance between two sites on the substrate and increases slowly. At the later time of our simulation, the curves of $G(r)$ tend to overlap. This result shows that the roughness of the RD model with thermal activation at high temperature do not increase indefinitely as in the RD model but it will saturate at the long time.

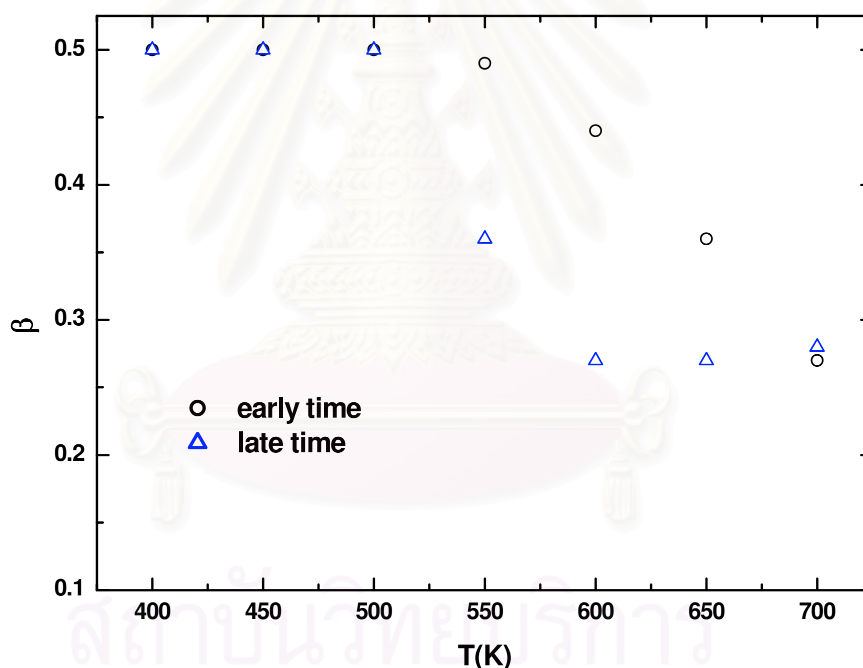

Figure 4.18: Plot of the growth exponent β at the early time and the late time versus the substrate temperature T for the RD model with thermal activation, calculated from Fig. 4.17

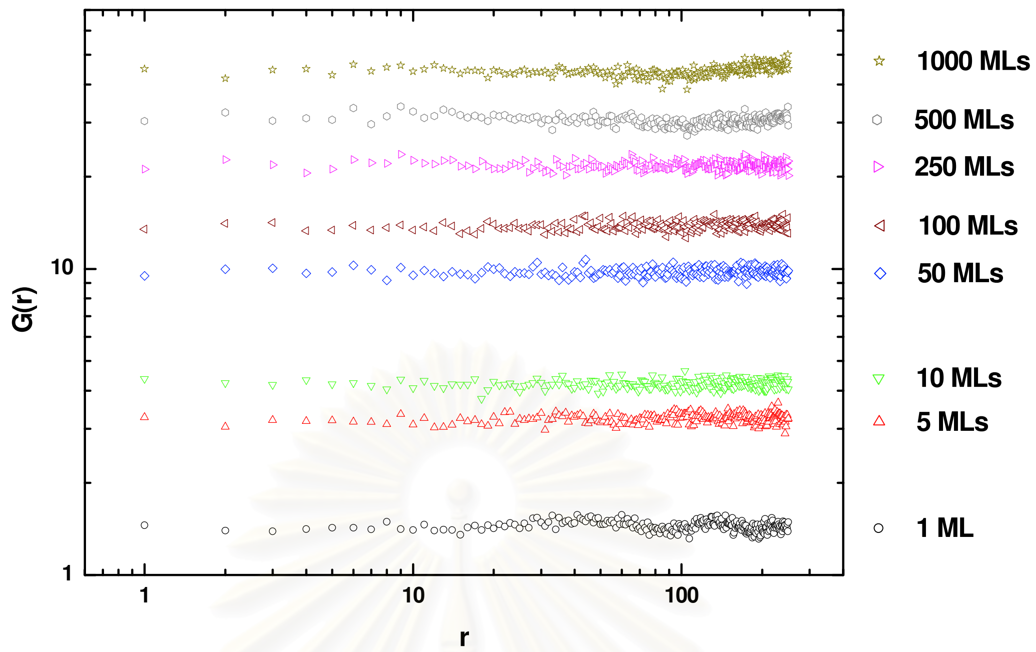

Figure 4.19: Plot of the height-difference correlation function $G(r)$ versus r for various t in the RD model with thermal activation at $T = 400$ K for the substrate size $L = 500$.

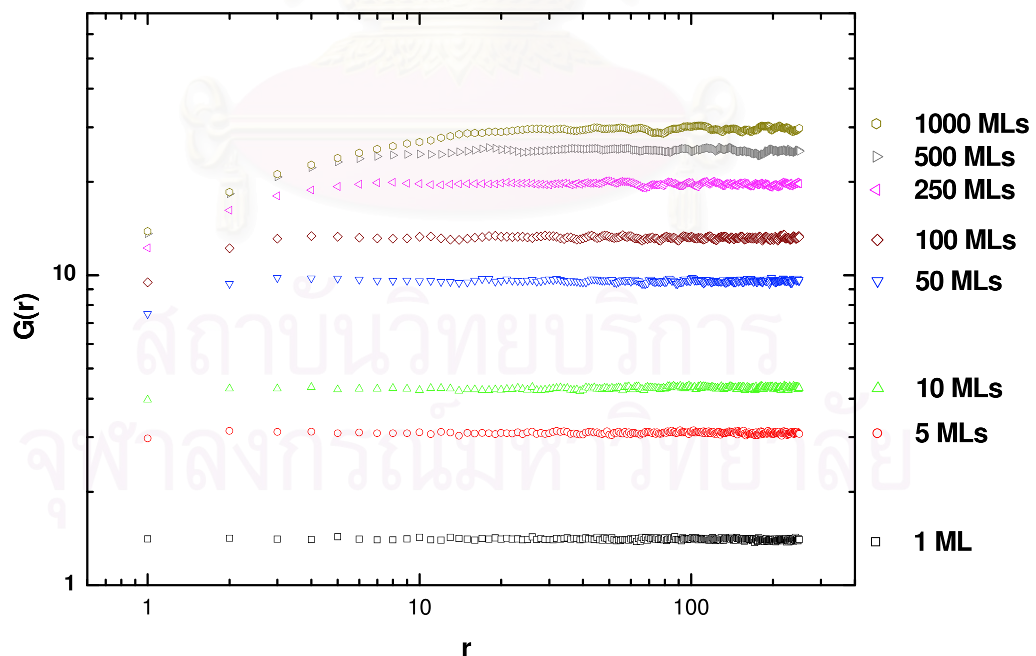

Figure 4.20: Plot of the height-difference correlation function $G(r)$ versus r for various t in the RD model with thermal activation at $T = 550$ K for the substrate size $L = 500$.

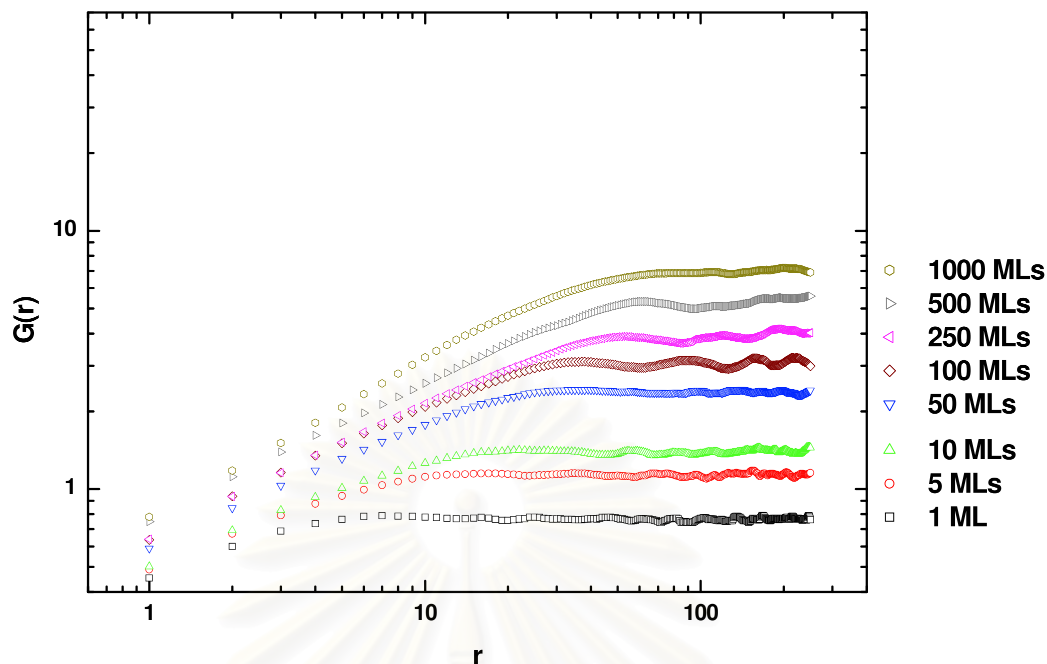

Figure 4.21: Plot of the height-difference correlation function $G(r)$ versus r for various t in the RD model with thermal activation at $T = 700$ K for the substrate size $L = 500$.

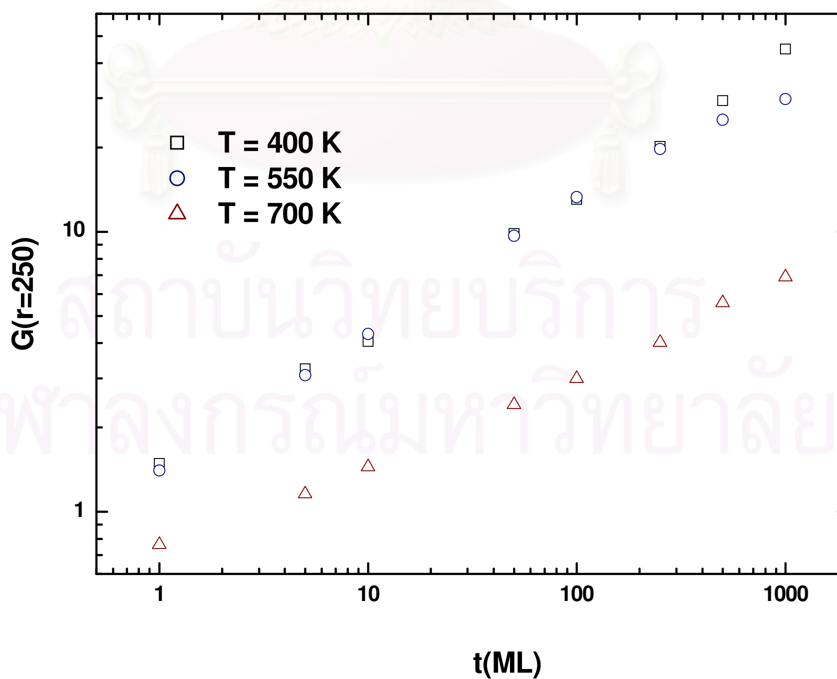

Figure 4.22: Plot of the height-difference correlation function $G(r)$ versus t on a log-log scale at $r = 250$ and $T = 400$, 550, and 700 K in the RD model for the substrate size $L = 500$.

4.3 Ballistic Deposition (BD) Model

Ballistic Deposition (BD) model is a simple model that omits the SOS condition during the deposition process. An atom is dropped randomly and incorporates on the film at a first point of contact with the growing aggregate. A surface height of the film depends on the height of the nearest-neighbor sites. The surface diffusion process and the desorption processes are neglected in this model. The void defects can be created because the SOS condition is not satisfied here.

The plot of height $h(x)$ versus the column site x which shows the surface morphology of the BD model for a system with substrate size $L = 500$ and at the time $t = 50$ MLs and $t = 500$ MLs is presented in Figs. 4.23(a) and (b) respectively. It is obvious that there are fluctuations in the surface. However, the surface morphology of the BD model is relatively smooth when compares with the surface of the RD model. To compare the surface morphologies, the plot of height $h(x)$ versus column site x of films from the RD model and the BD model are shown together in Fig. 4.24. Although, the surface morphology of the BD model is smoother than the RD model, the volume of the BD film is not conserved. After growing 500 MLs on a substrate of size $L = 500$, the average height of the film from the BD model is approximately 1060 MLs. This is much thicker than the film grown by the RD model which has the average height of 500 MLs as expected. The simulated schematic diagram which shows the position of the atoms in the film, Fig. 4.25, shows that there are the void defects with a variety of sizes and shapes in the film. This result shows that the void defect can be created because the atom is deposited without the SOS condition. To study the void defect, we plot the defect density $D(t)$ as a function of the time t for $L = 500$ in Fig. 4.26. $D(t)$ rapidly increases and reaches the value of about 0.52. This means over half of the bulk is an empty space.

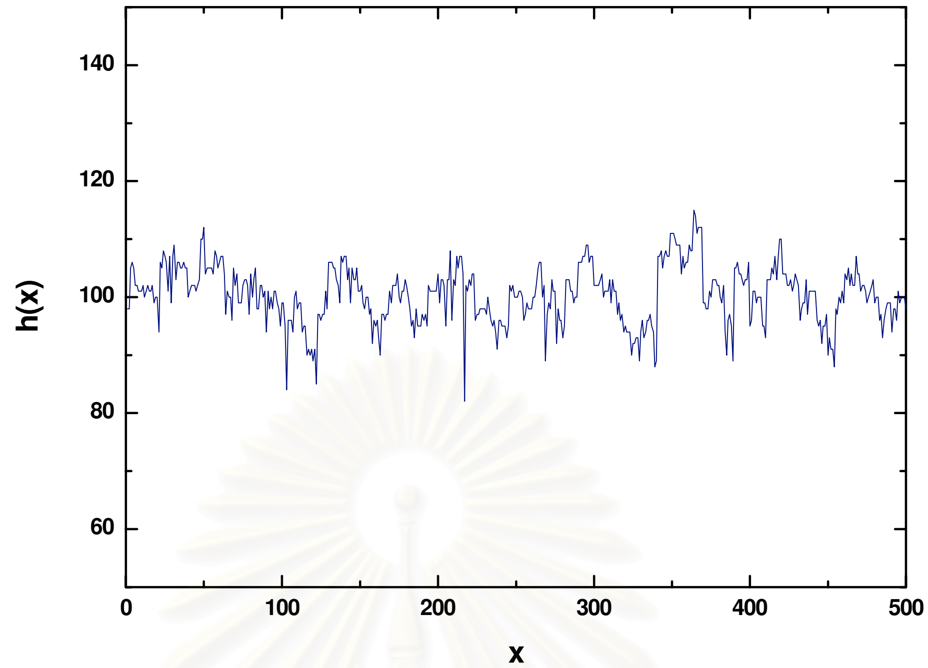

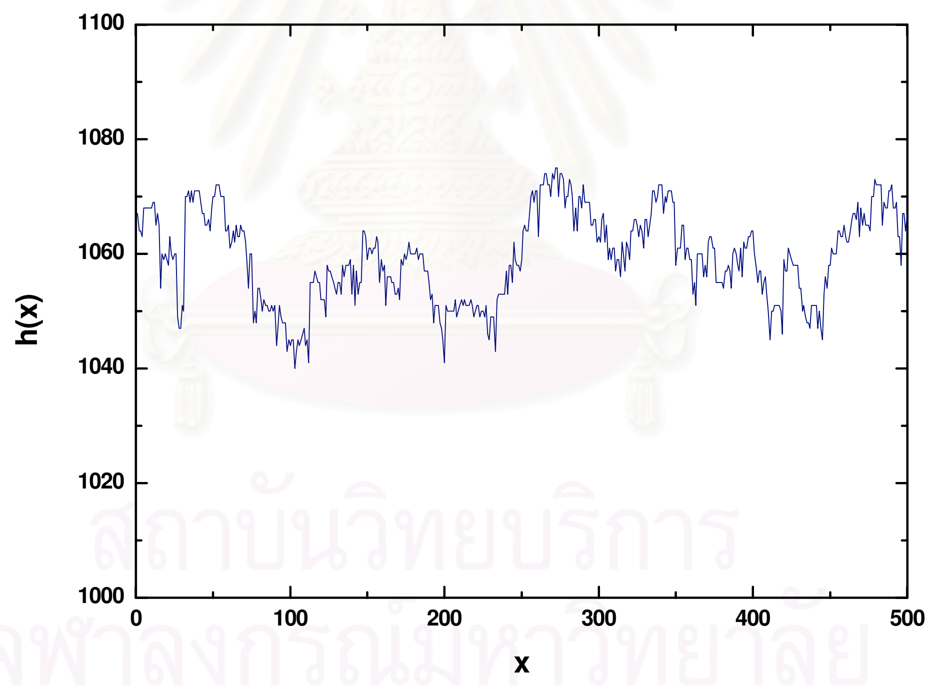

Figure 4.23: Plot of the height $h(x)$ versus x of the BD model on the substrate size $L = 500$ at 50 MLs (a) and 500 MLs (b)

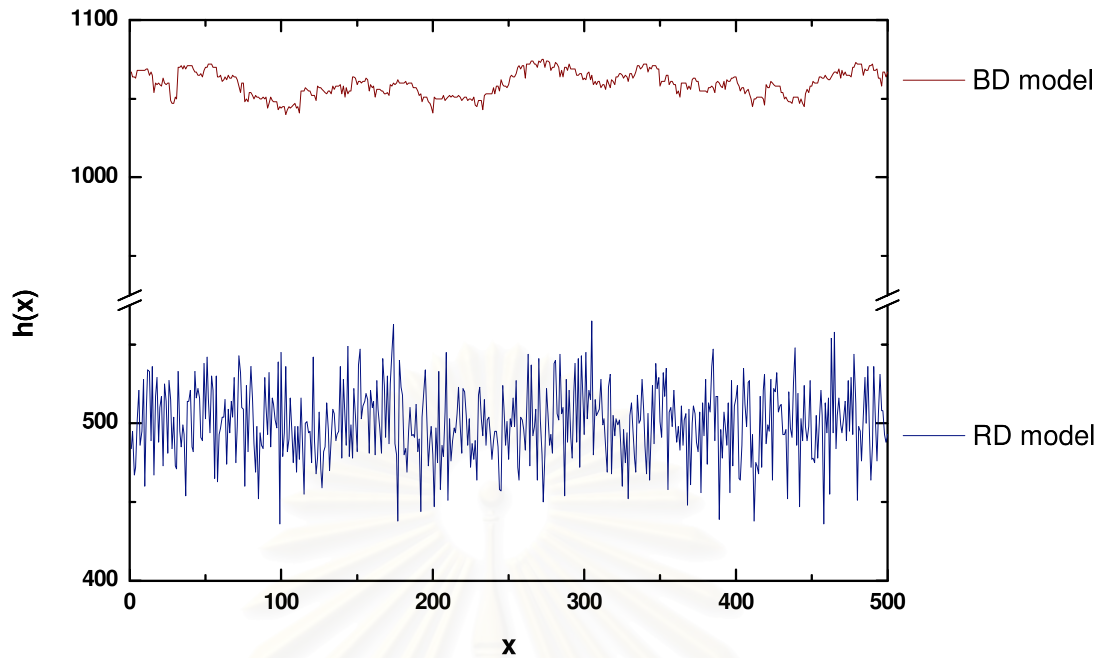

Figure 4.24: Plot of the height $h(x)$ versus x of the BD model compares with the RD model at 500 MLs on the substrate size $L = 500$.

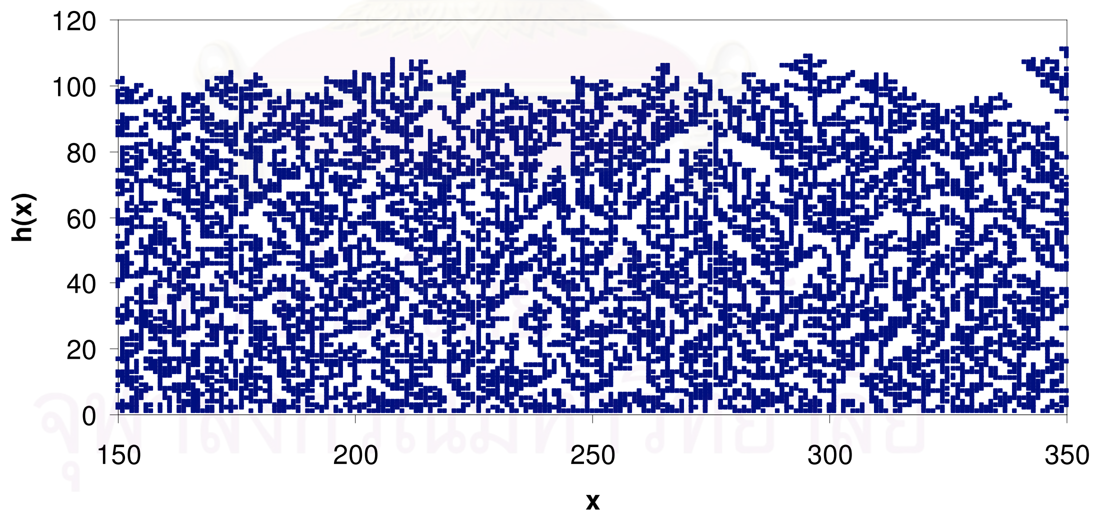

Figure 4.25: The simulated schematic diagram of the BD model at $t = 50$ MLs for the substrate size $L = 500$ expands view of $x = 150 - 350$.

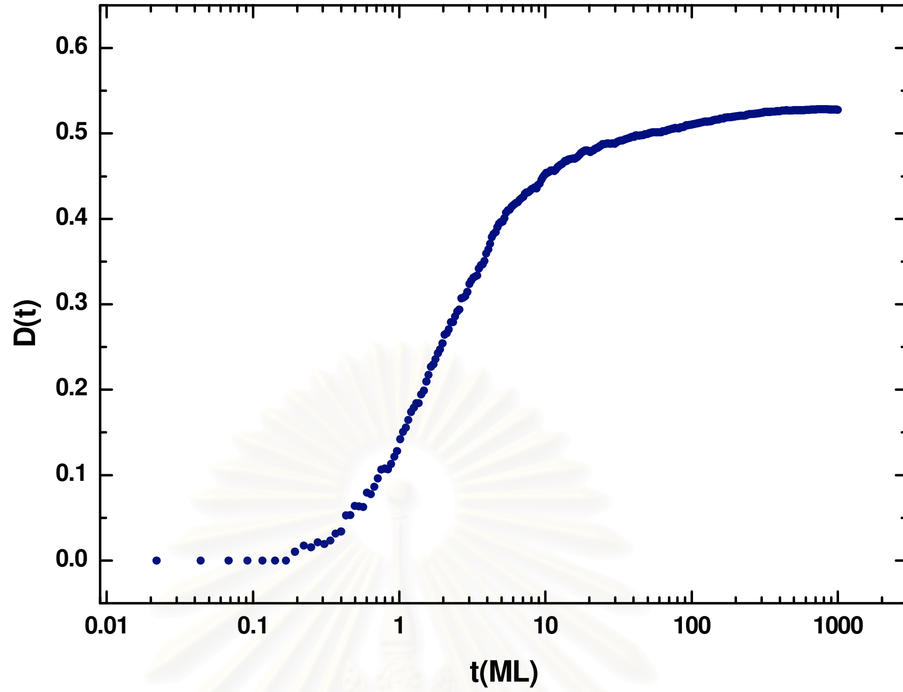

Figure 4.26: Plot of the defect density $D(t)$ versus the log time t in the BD model for the substrate size $L = 500$.

Fig. 4.27 shows a plot of interface width $W(t)$ versus the time t on log-log scale of the BD model for $L = 500$. At very early time ($t < 0.2$ MLs), $W(t)$ increases as the power of t with a slope ~ 0.5. This growth exponent β indicates that the growth process is random, similar to the behavior of early time $W(t)$ in the RD model with thermal activation model. This can be explained in the samefashion as in the previous section. When looking at the void defect density results in Fig. 4.26, it can be seen that $D(t < 0.2$ MLs$) \approx 0$, implying that there is no void defect in the early time. This is because in the very early time there are very few incorporated atoms and so the newly deposited atom does not have anything to overhang to. As a result, the film grows independently as the RD model. After this early time regime, β decreases to ~ 0.26 which is lower than β in the RD model. The straight line in Fig. 4.27 indicates the best fit which yields the value of β. This value shows that the roughness of the BD model increases slower than the RD model. A plot of the height-difference correlation function $G(r)$ versus the distance r from $t = 1$ ML to $t = 1000$ MLs is shown in Fig.

4.28. We found that $G(r)$ increases as a power of r and eventually the value of the correlation function saturates. This is because the height of the film depends on the nearest-neighbor sites in the deposition process. A plot of $G(r)$ versus t at $r = 250$ is show in 4.29. We also found that the value of $G(r)$ increases when t increases. The overlap of curves at the large time, shown in Fig. 4.28, shows that the difference of the height between the two sites do not increase indefinitely as in the RD model. This result shows that the roughness of the BD model do not increase indefinitely with time but it will saturate at the large time.

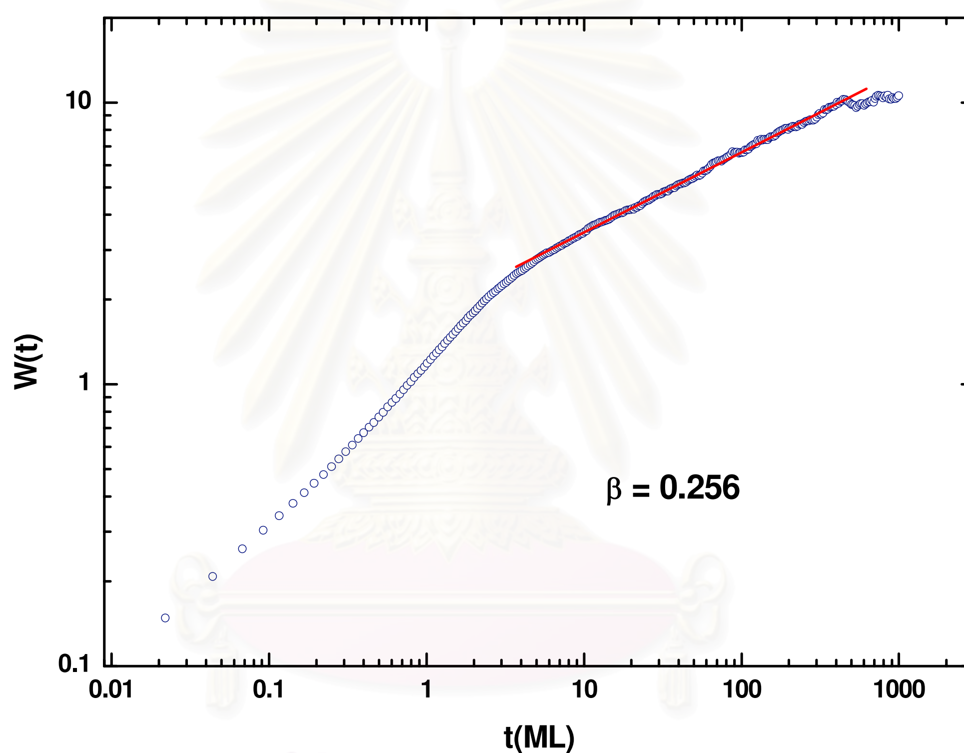

Figure 4.27: Plot of the interface width $W(t)$ versus the time t on a log-log scale of the BD model for the substrate size $L = 500$.

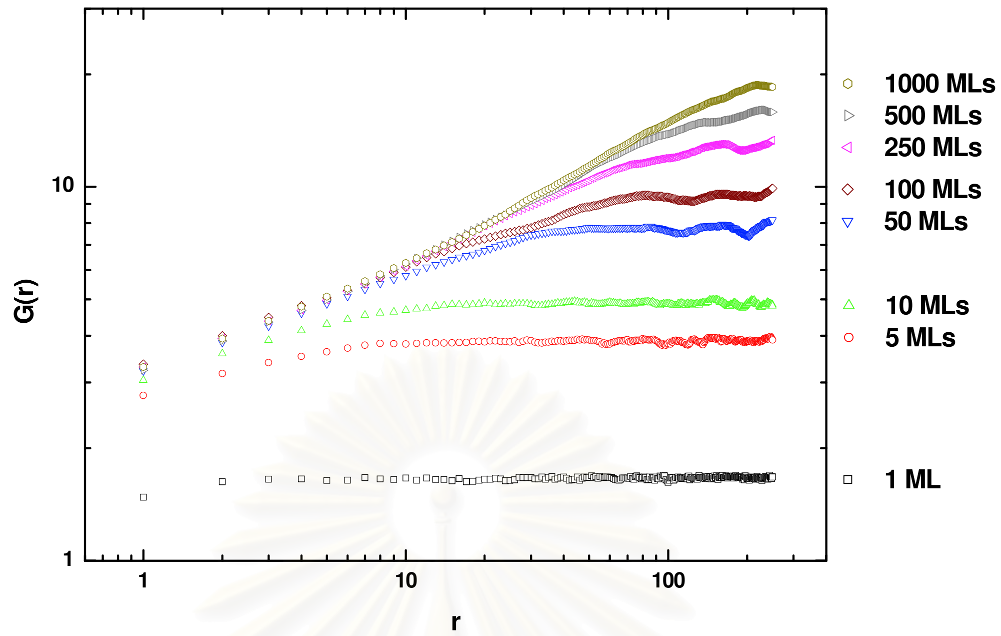

Figure 4.28: Plot of the height-difference correlation function $G(r)$ versus r on log-log scale for various t in the BD model for the substrate size $L = 500$.

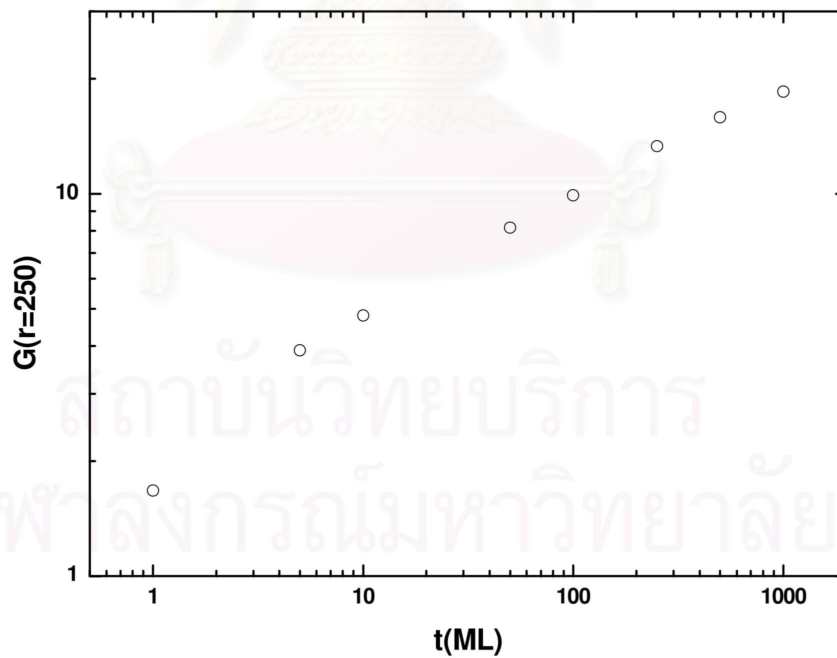

Figure 4.29: Plot of the height-difference correlation function $G(r)$ versus t on a log-log scale at $r = 250$ in the BD model for the substrate size $L = 500$.

สถาบันวิทยบริการ
จุฬาลงกรณ์มหาวิทยาลัย

4.4 Ballistic Deposition (BD) Model with Thermal Activation

Ballistic Deposition (BD) model with thermal activation is based on the BD model. In this model, the deposition rule obeys the BD model. The SOS condition is not satisfied in this process which is different from the RD model with thermal activation. After deposited, a surface atom can diffuse continuously. The SOS condition is not applied in the diffusion process either. As a result, the void defect can be formed in both the deposition and diffusion process. The hopping rate is calculated through the Arrhenius expression which depends on the substrate temperature and the configuration of the surface atom.

To observe an effect of the substrate temperature T on the morphology, we show the plots of the height fluctuation versus x of the substrate size $L = 500$ with the thickness 50 MLs when the substrate temperature ranges from $T = 400$ K to $T = 700$ K in Fig. 4.30. The simulated schematic diagrams which show the position of the atoms corresponding to theses films are shown in ranges from Figs. 4.31 - 4.36. At low temperature, many small fluctuations and spikes can be observed in the surface morphology. There are small size of voids spreading over the bulk. When the temperature increases, the surface morphology becomes smoother. The number of small void decreases and coalesces into large void. The film seems to be smooth and compact at high temperature ($T = 700$ K). A plot of the defect density $D(t)$ with the time t at the substrate temperature $T = 400$, 500, 550, 600, 650 and 700 K for $L = 500$ is shown in Fig. 4.37. The plot of the defect density at $t = 50$ MLS versus the substrate temperature is also shown in Fig. 4.38. $D(t)$ increases rapidly with t and eventually saturates at $D(t) \leq 0.52$. It was also found that the defect density decreases when the substrate temperature is increased. At $T = 400$ K, the saturate defect density is ~ 0.52 while it falls to ~ 0.01 at $T = 700$ K. From the results at low temperature, the properties of the film is similar to the BD model. This is because the hopping rate is very small at low temperature. The atom is deposited according to the deposition rule of the BD model and has small probability to diffuse. As a result, The film shows the same properties as the BD model. At higher temperature, the surface atom has

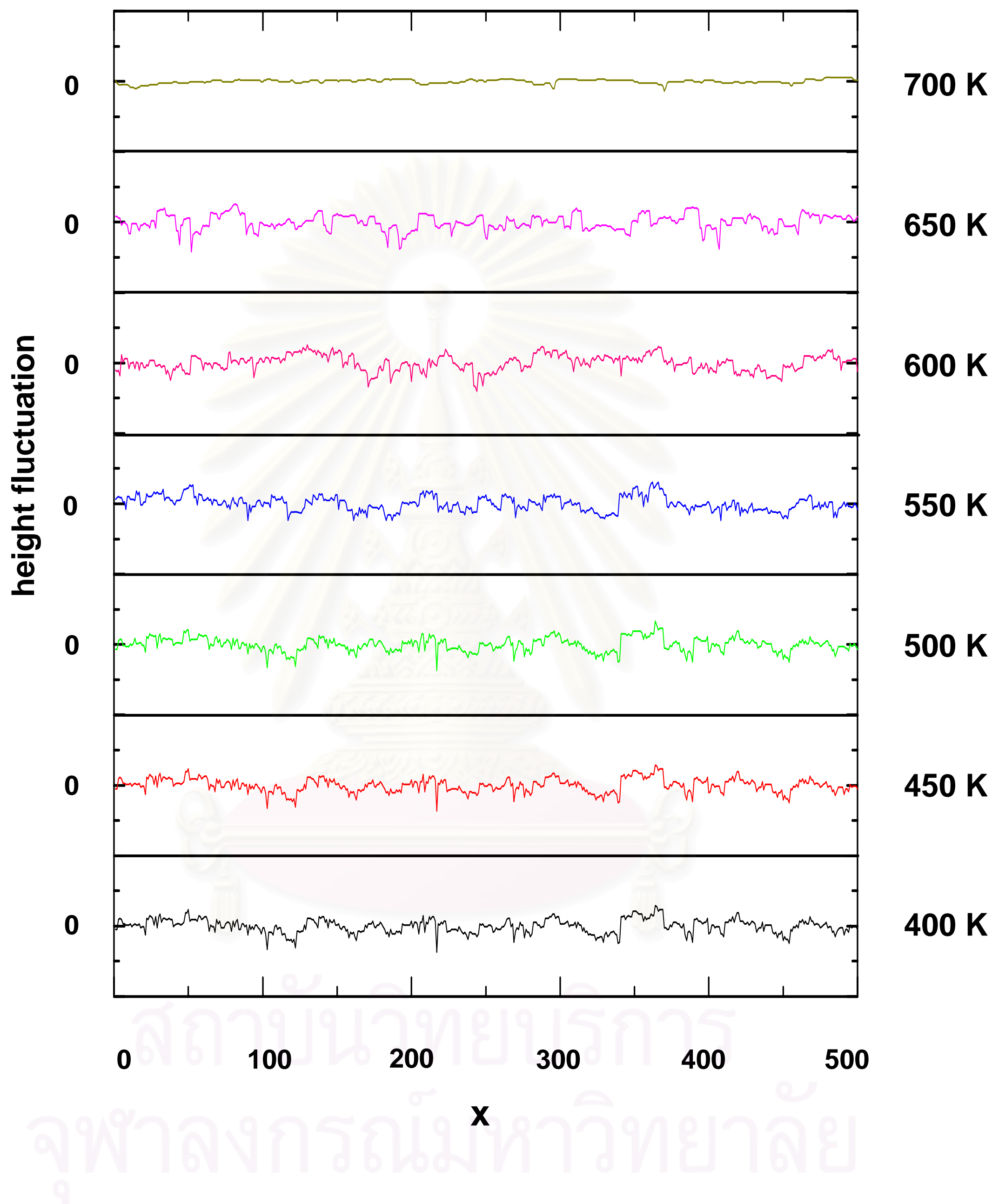

Figure 4.30: Plot of the height fluctuation versus x of the BD model with thermal activation at $T = 400$, 450, 500, 550, 600, 650 and 700 K for $t = 500$ MLs on the substrate size $L = 500$.

higher probability to diffuse. The atom which diffuses to the kink site will remain at that site for a long time because at this site it has very low probability to diffuse. The small voids and gaps are filled by the surface atoms. As a result, the film becomes smoother. The number of small void decreases and coalesces into the large void as T increases. At high temperature, the atom has high hopping rate and can diffuse to rearrange the formation in layer-by-layer mode, which decreases the void formation. As a result, the film is smooth and the defect density is very low.

We plot the interface width $W(t)$ at $T = 400 - 700$ K as a function of the time t for $L = 500$ in Fig. 4.39. The results show that the interface width of each system increases with time. In very early time ($t \leq 0.1$ MLs), the slope of $W(t)$ is ~ 0.5. This slope shows the random growth in the early time which is the same as in the BD model. After this regime, we found that $W(t)$ behaves the same as in the BD model for the low temperature ($T < 600$ K). At higher temperature, the slope of $W(t)$ decreases when T increases before it behaves the same as in the BD model, $\beta \sim 0.26$, at the latest simulation time. This is because the hopping rate is very low at low temperature. The surface atom cannot diffuse much. As a result, the film shows roughness behavior which is same as the BD model. For high temperature, the hopping rate is high. The film has rarely kink sites which trap the deposited and diffused atom at the early time. The surface atom can diffuse long distance to find a suitable site before it is trapped. As a result, β decreases as T increases in the early time regime. For the latest time, there are more fluctuations with large amplitude. This leads to the increase of the kink sites on the film. When the temperature increases, the surface has high probability to diffuse but there are many kink sites on the film. The surface atom is trapped easily. The surface atom cannot diffuse long distance to find a suitable site. With more fluctuations with large amplitude, the deposited atom is easy to overhang following the deposition rule of the BD model. As a result, the slope of $W(t)$ is the same as in the BD model for the latest time. It is also found that the change of $D(t)$ in time corresponds with the change $W(t)$ in time. From Fig. 4.37, the temporal change in $D(t)$ of $T = 600$ K at $t \sim 100$ MLs corresponds to the change in $W(t)$

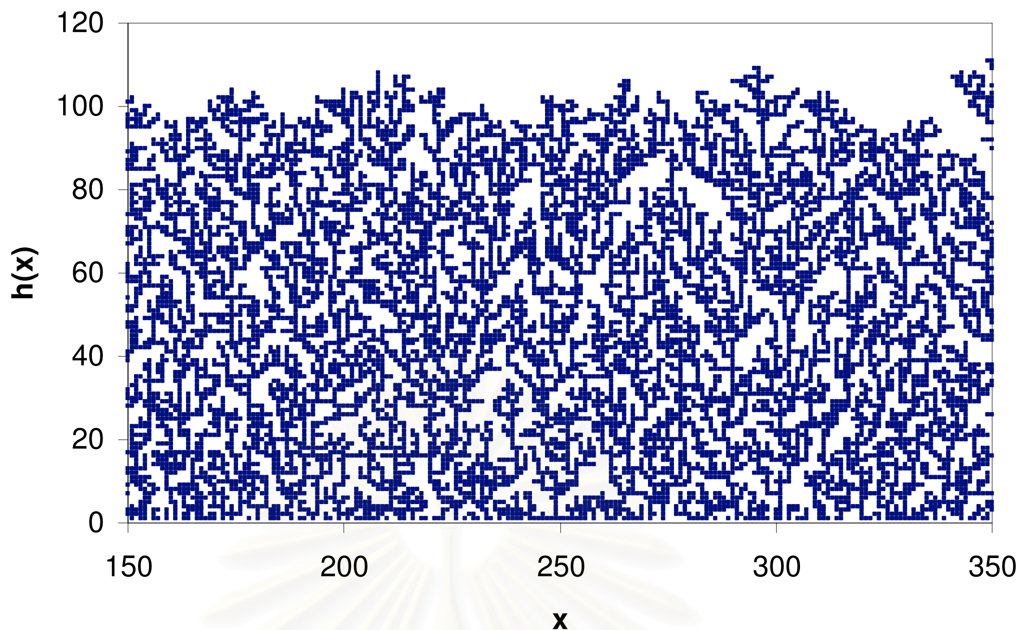

Figure 4.31: The simulated schematic diagram of the BD model with thermal activation for $T = 400$ K and the substrate size $L = 500$ at $t = 50$ MLs expands view of $x = 150 - 350$.

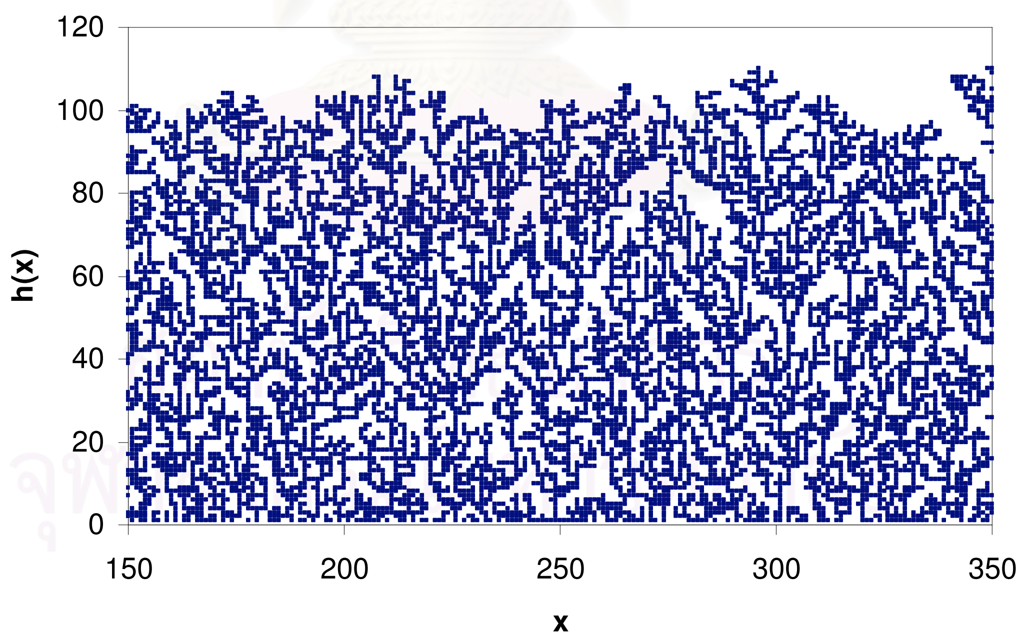

Figure 4.32: The simulated schematic diagram of the BD model with thermal activation for $T = 500$ K and the substrate size $L = 500$ at $t = 50$ MLs expands view of $x = 150 - 350$.

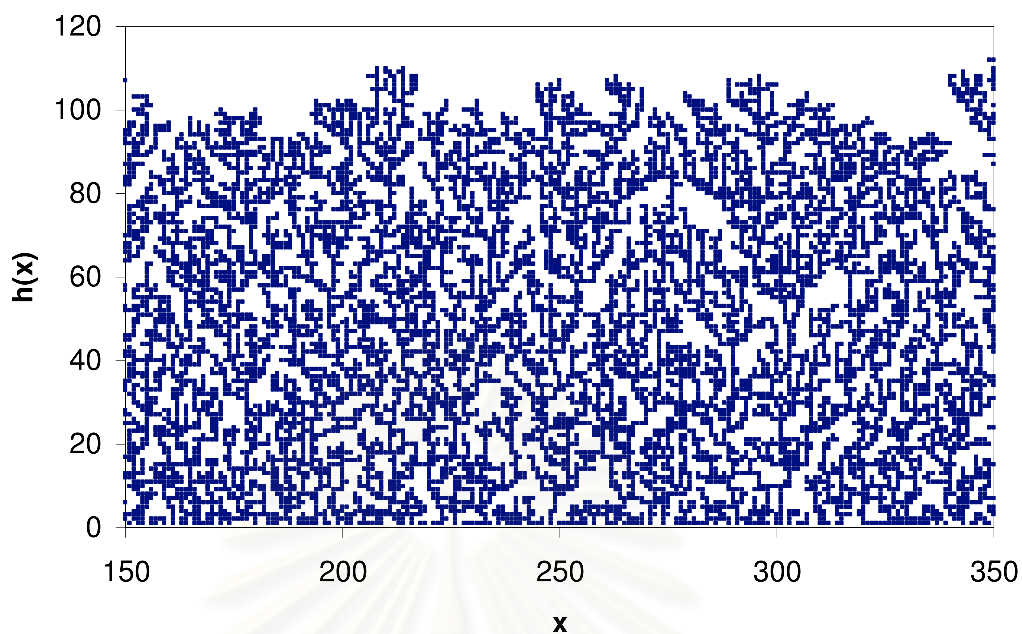

Figure 4.33: The simulated schematic diagram of the BD model with thermal activation for $T = 550$ K and the substrate size $L = 500$ at $t = 50$ MLs expands view of $x = 150 - 350$.

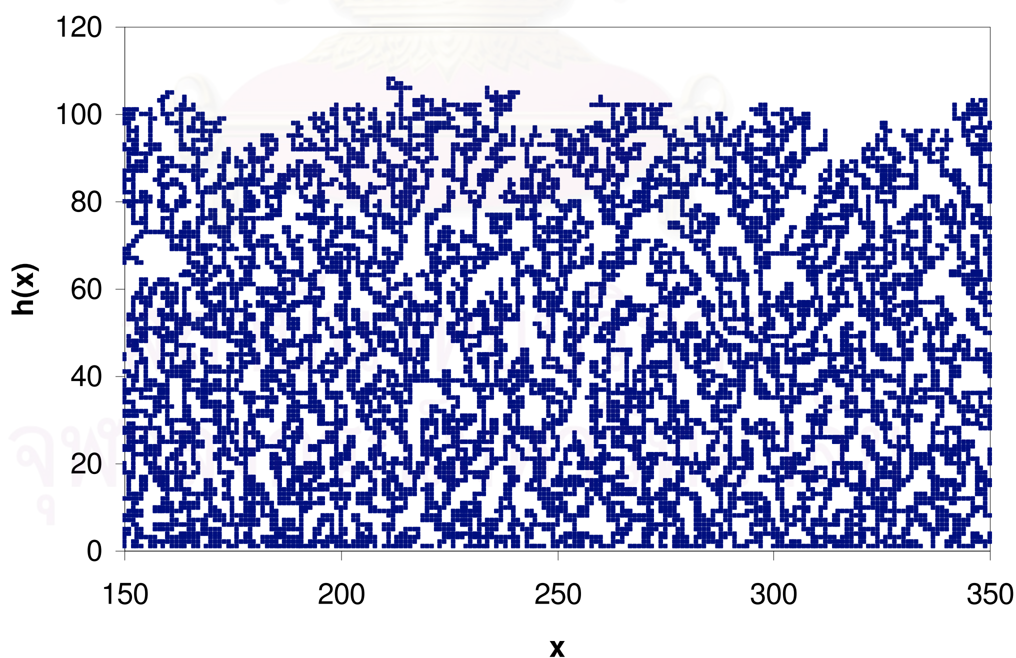

Figure 4.34: The simulated schematic diagram of the BD model with thermal activation for $T = 600$ K and the substrate size $L = 500$ at $t = 50$ MLs expands view of $x = 150 - 350$.

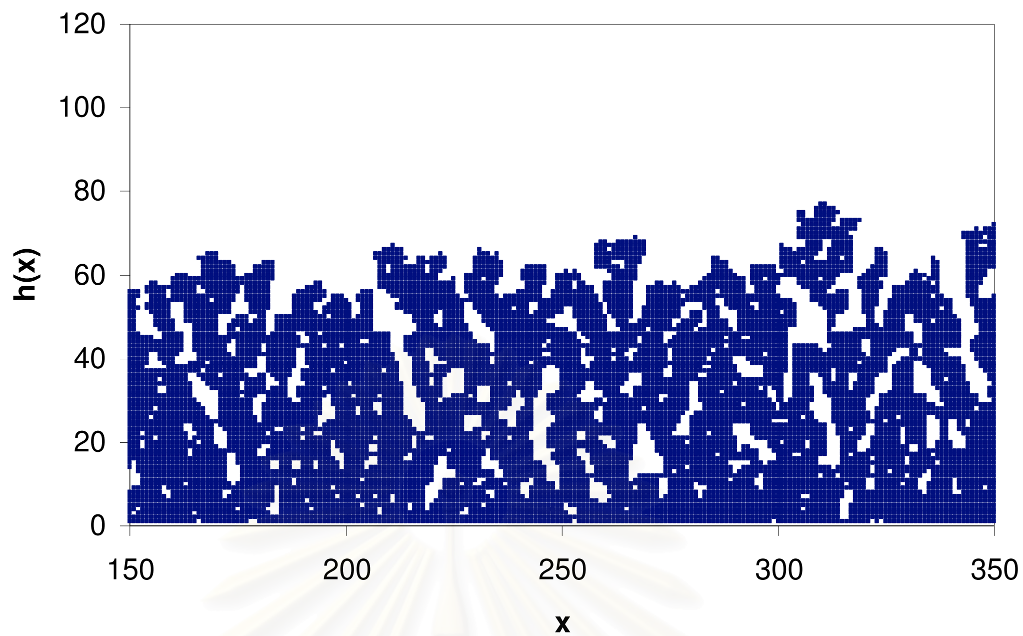

Figure 4.35: The simulated schematic diagram of the BD model with thermal activation for $T = 650$ K and the substrate size $L = 500$ at $t = 50$ MLs expands view of $x = 150 - 350$.

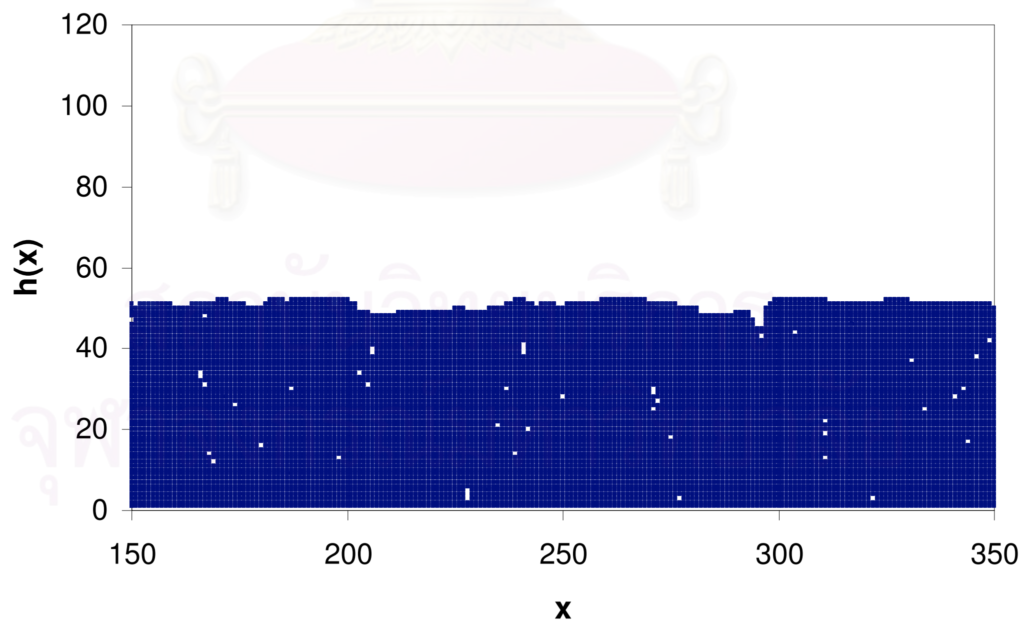

Figure 4.36: The simulated schematic diagram of the BD model with thermal activation for $T = 700$ K and the substrate size $L = 500$ at $t = 50$ MLs expands view of $x = 150 - 350$.

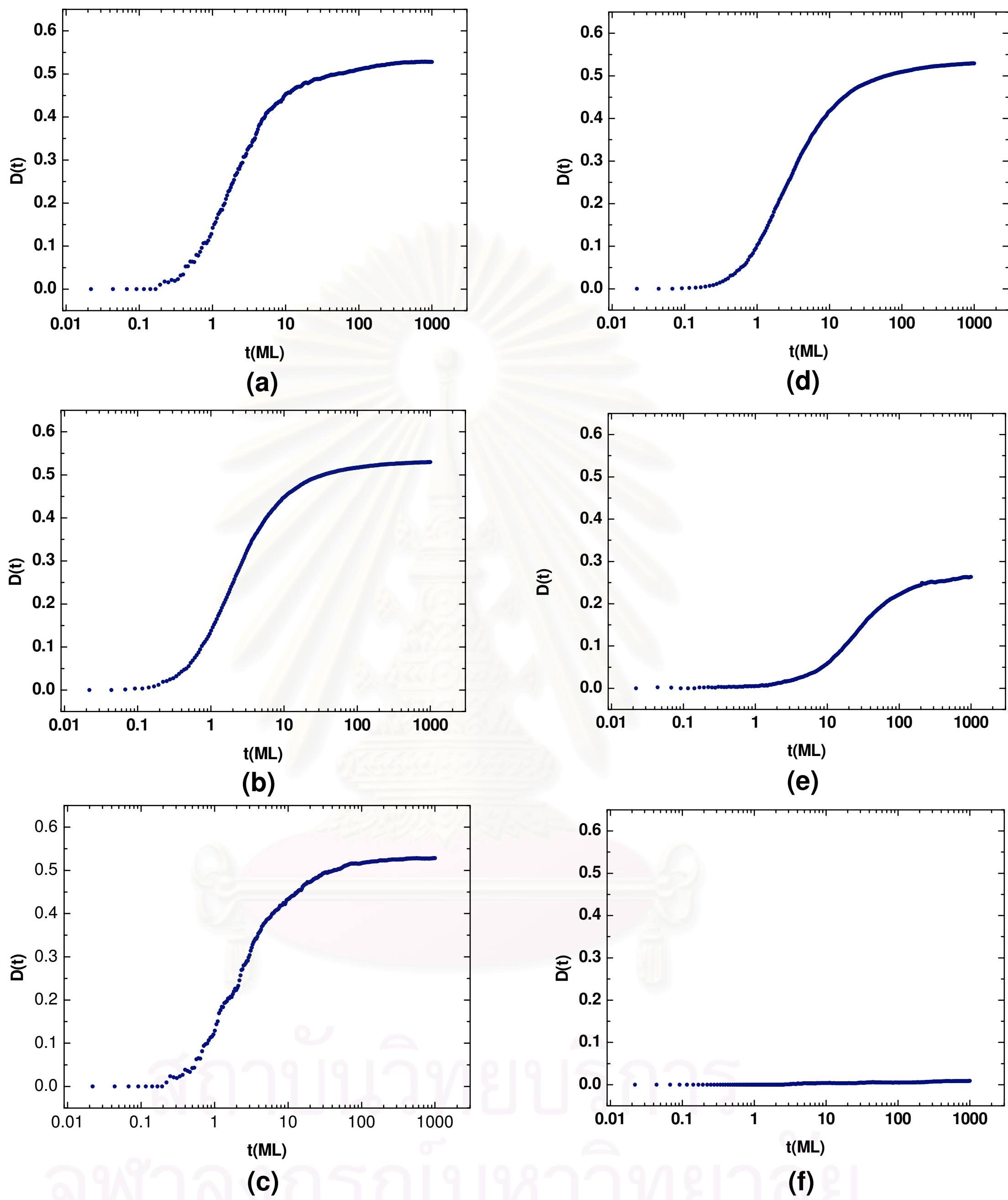

สถาบันวิทยบริการ
จุฬาลงกรณ์มหาวิทยาลัย

Figure 4.37: Plot of the defect density $D(t)$ versus the log time t in the BD model with thermal activation model for various T on the substrate size $L = 500$ (a) $T = 400$ K, (b) $T = 500$ K, (c) $T = 550$ K, (d) $T = 600$ K, (e) $T = 650$ K and (f) $T = 700$ K.

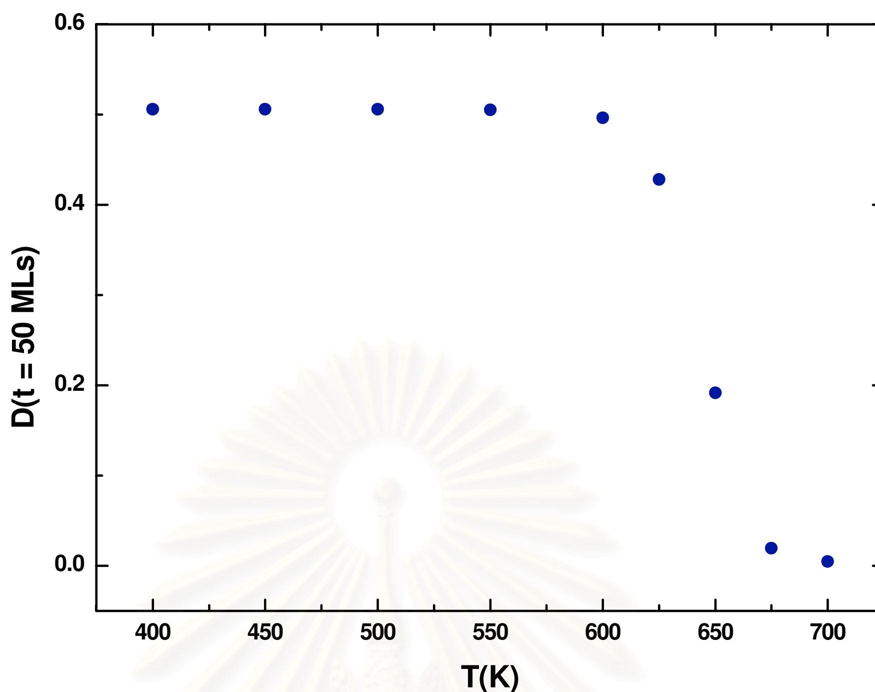

Figure 4.38: Plot of the defect density $D(t)$ versus the substrate temperature T in the BD model with thermal activation model on the substrate size $L = 500$ at $t = 50$ MLs.

We show the height-difference correlation function $G(r)$ at $t = 1$ to $t = 1000$ ML in Figs. 4.40- 4.42. We also show the plot of $G(r)$ versus t at $r = 250$ and the substrate temperature $T = 400$, 550, and 700 K on log-log scale is show in Fig. 4.43. At low temperature ($T \leq 550$ K), $G(r)$ increases as power of r and eventually the value of the correlation function saturates. It is also obvious that the value of $G(r)$ increases when t increases and there are overlap of the curves at large time. This results show the same behavior as in the BD model because the hopping rate is very small. At high temperature ($T = 700$ K), the surface atom has high probability to diffuse due to high hopping rate. $G(r)$ do not show the same behavior as in the BD model but it is similar in the RD model with thermal activation at high temperature. This result shows that the behavior of the BD model with thermal activation is different from the BD model at high temperature.

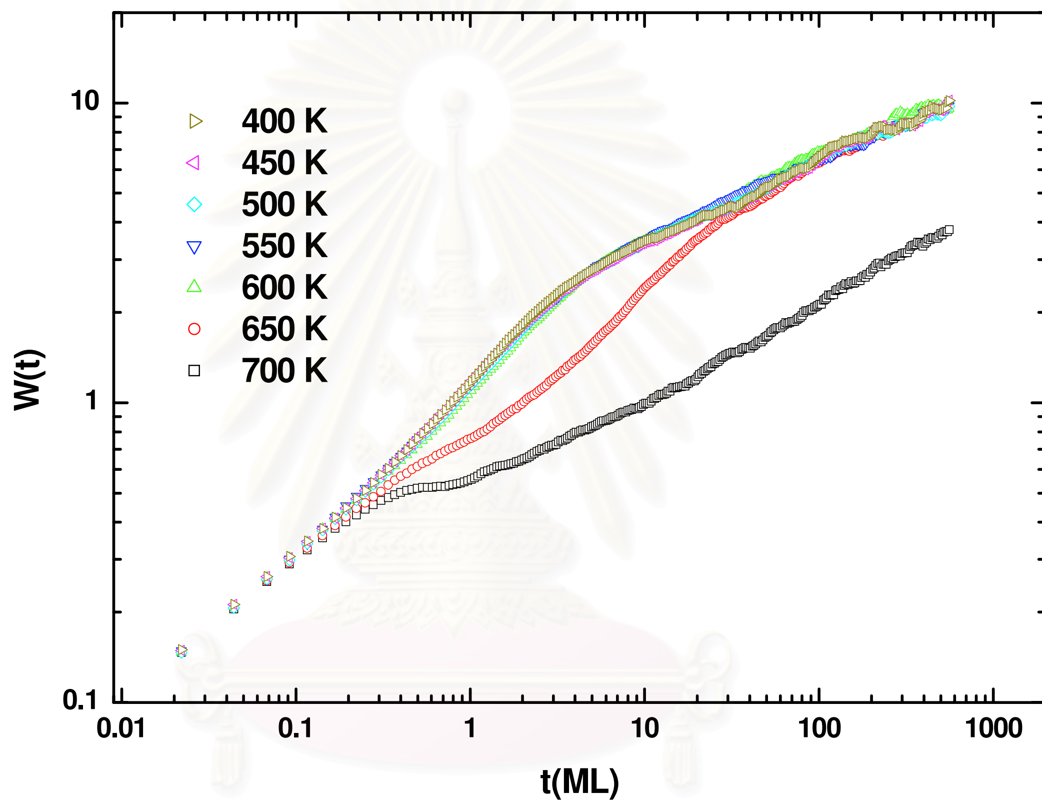

Figure 4.39: Plot of the interface width $W(t)$ versus the time t on a log-log scale of the RD model with thermal activation for the substrate size $L = 500$ at $T = 400$, 450, 500, 550, 600, 650 and 700 K.

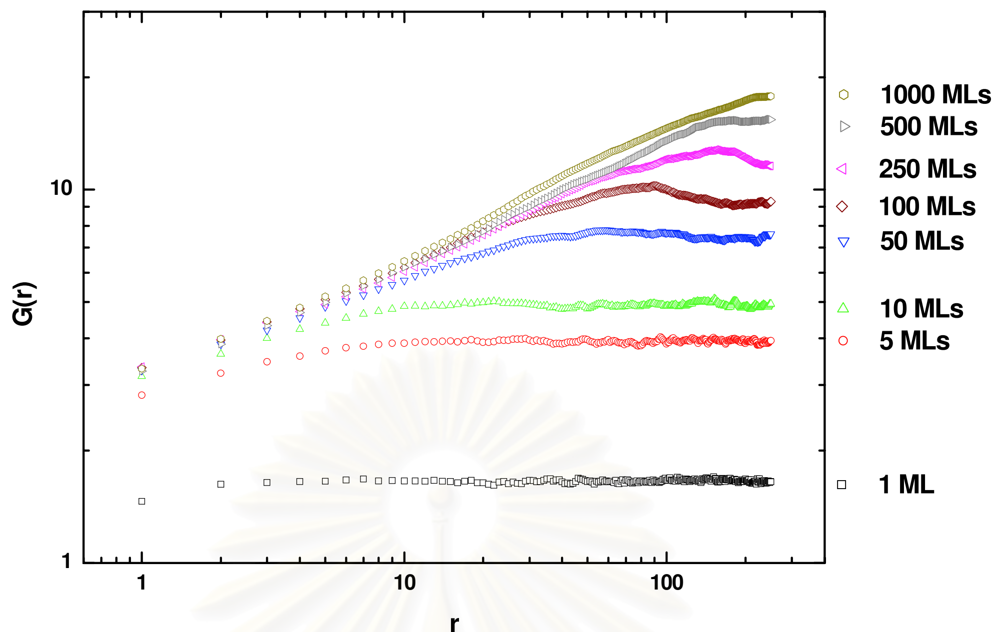

Figure 4.40: Plot of the height-difference correlation function $G(r)$ versus r for various t in the BD model with thermal activation at $T = 400$ K for the substrate size $L = 500$.

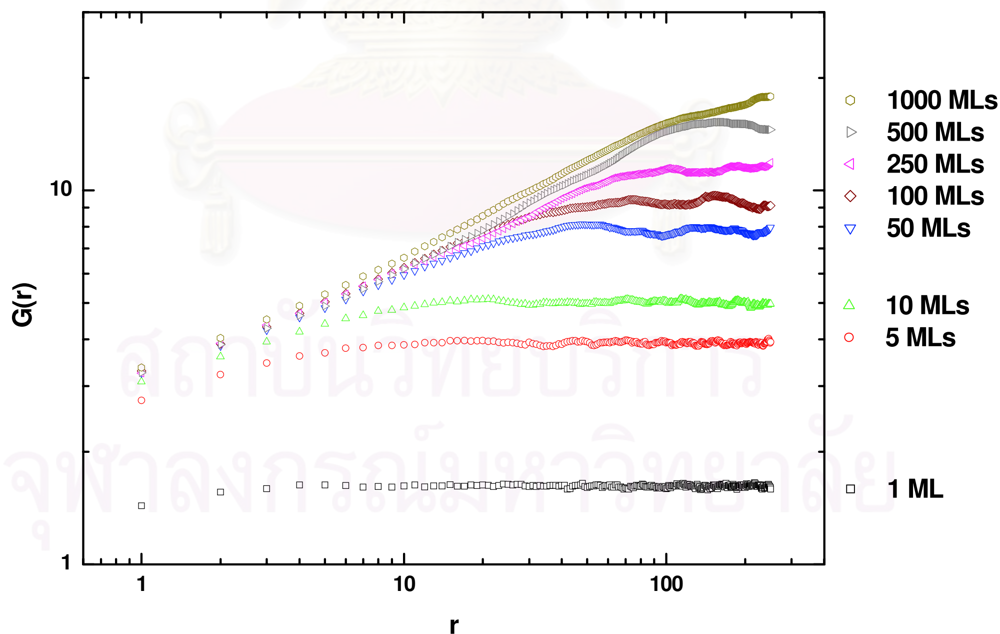

Figure 4.41: Plot of the height-difference correlation function $G(r)$ versus r for various t in the BD model with thermal activation at $T = 550$ K for the substrate size $L = 500$.

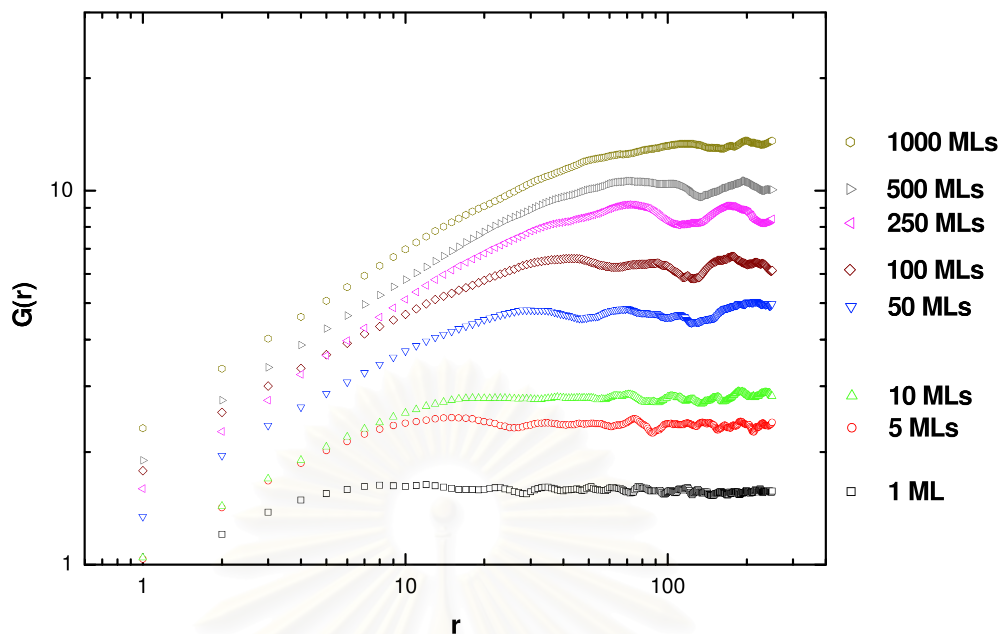

Figure 4.42: Plot of the height-difference correlation function $G(r)$ versus r for various t in the BD model with thermal activation at $T = 700$ K for the substrate size $L = 500$.

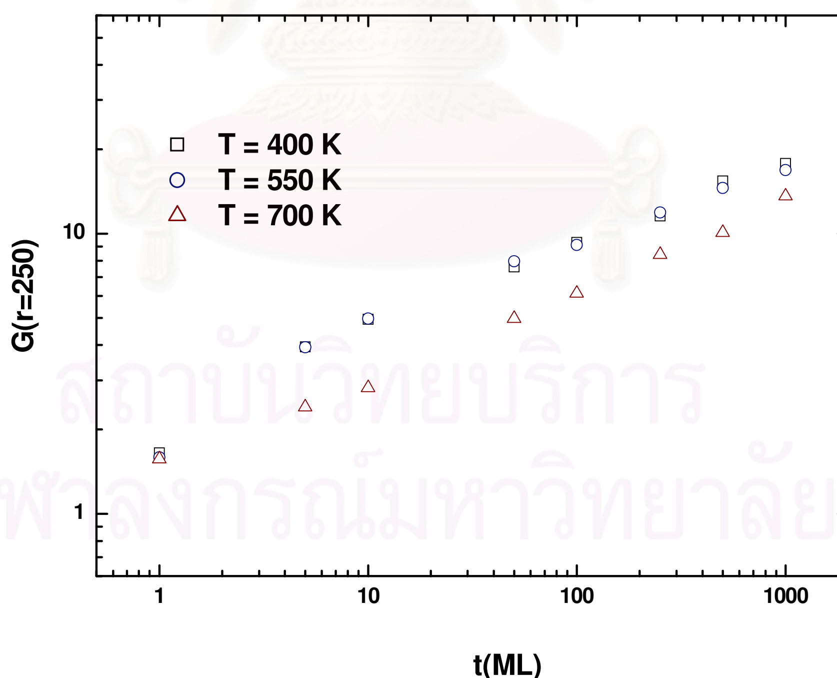

Figure 4.43: Plot of the height-difference correlation function $G(r)$ versus t on a log-log scale at $r = 250$ and $T = 400$, 550, and 700 K in the BD model for the substrate size $L = 500$.

4.5 Discussions

In this chapter, we show the simulation results of our discrete models, the RD model with thermal activation and the BD model with thermal activation. The two models are different only in the deposition process. The deposition rule of the RD model with thermal activation obeys the SOS condition while this condition is not used in the BD model with thermal activation.

From our results, at low substrate temperature, the hopping rate is very small. As a result, the surface atom has low probability to diffuse. The BD model with thermal activation shows a distinctive behavior as compare to the RD model with thermal activation. From the plot of the height fluctuation of the RD model with thermal activation compares with the BD model with thermal activation for the substrate size $L = 500$ with the thickness 50 MLs at the substrate temperature $T = 500$ K which is shown in Fig. 4.44 (a), the surface morphology of BD model with thermal activation is smoother than the RD model with thermal activation which has many large fluctuations in height. The defect density of both models usually increases with the growth time. A plot of the defect density $D(t)$ versus substrate temperature of the RD model with thermal activation model compares with the BD model with thermal activation at $t = 50$ MLs in Fig. 4.45 shows that the defect density the RD model with thermal activation increases as the substrate temperature increases while the defect density of the BD model with thermal activation decreases as the substrate temperature increases. To comparing the roughness, we plot the interface width $W(t)$ versus the time t of of the BD model with thermal activation model compares with the RD model with thermal activation on the substrate size $L = 500$ at $T = 400$ K in Fig. 4.46 (a). This plot show that the roughness of both models usually increases with the growth time but the roughness of the BD model with thermal activation increases slower than that of the RD model with thermal activation. At high substrate temperature, the hopping rate is high. As a result, the surface has high probability to diffuse. These models show the same behavior. The plot of the height fluctuation of the RD model with thermal activation compares with the BD model with thermal activation at the substrate temperature $T = 700$ K which is shown in Fig. 4.44 (b) shows that

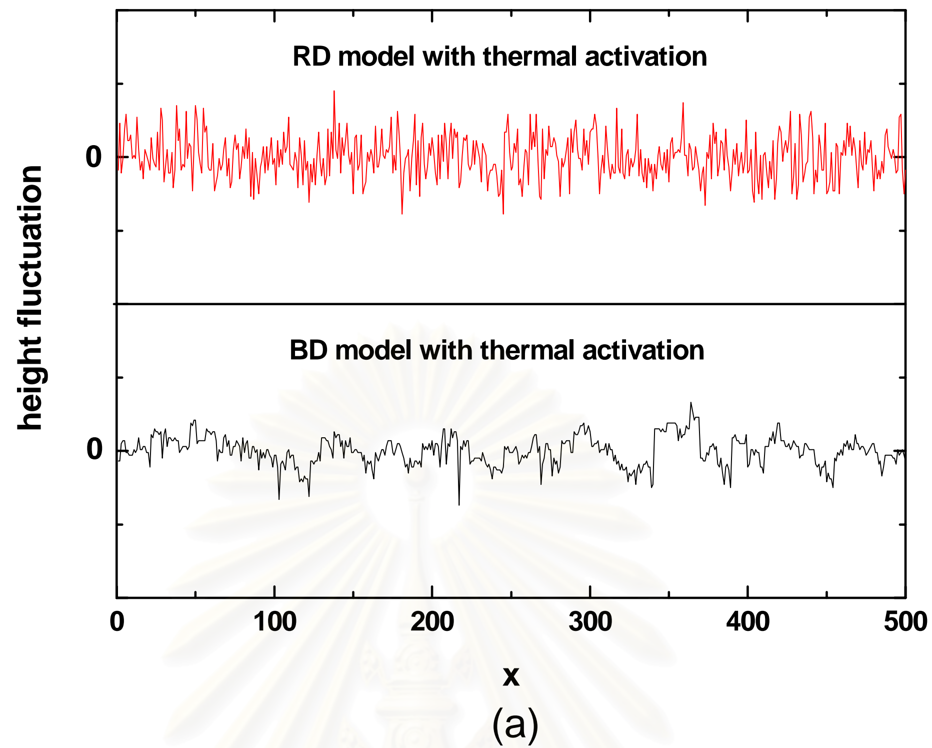

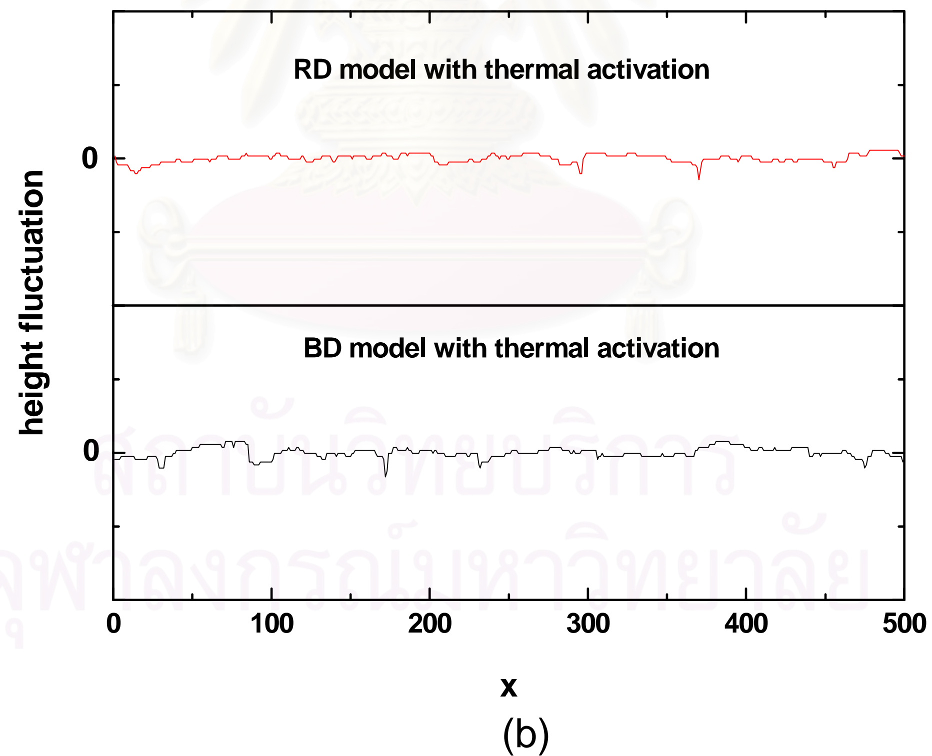

Figure 4.44: Plot of the height fluctuation versus x of the BD model with thermal activation compares with the RD model with thermal activation for the substrate size $L = 500$ with the thickness 50 MLs at the substrate temperature (a) $T = 500$ K and (b) $T = 700$ K.

the surface of both models becomes smoother when the substrate temperature increases. The void defect density which usually increases with the growth time decreases when the substrate temperature increases as shown in Fig. 4.45. The plot of the interface width $W(t)$ versus the time t of of the BD model with thermal activation model compares with the RD model with thermal activation at $T = 700$ K which is shown in Fig. 4.46 (b) shows that the roughness of both models show the same behavior. The roughness of the film increases slower when the substrate temperature increases. These results (except the defect density) agree with other models that use Arrhenius relation for the hopping rate [2, 4, 5, 16, 17].

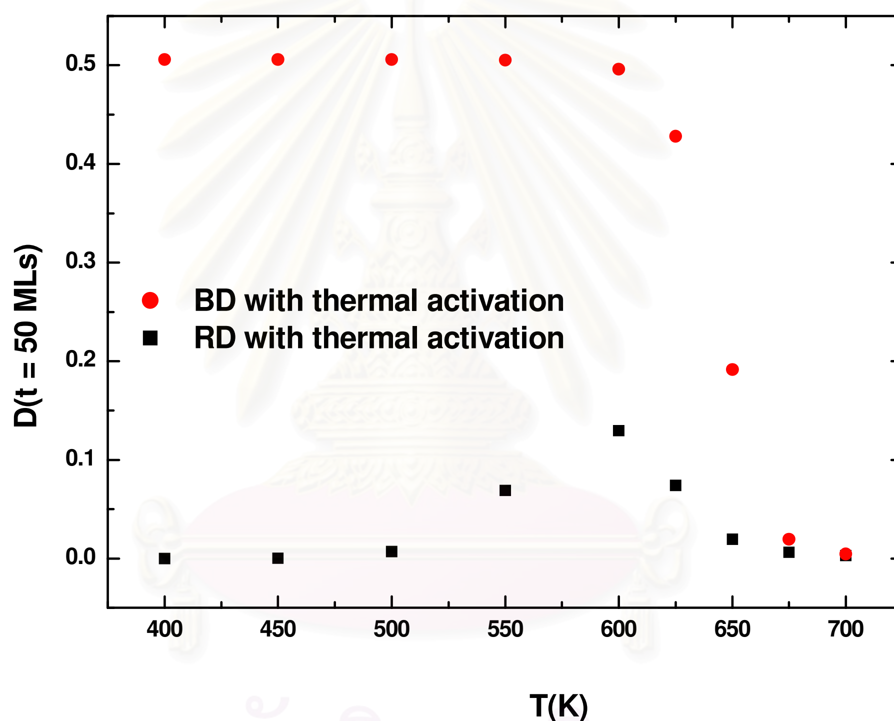

Figure 4.45: Plot of the defect density $D(t)$ versus the substrate temperature of the BD model with thermal activation model compares with the RD model with thermal activation on the substrate size $L = 500$ at $t = 50$ MLs.

Several experiments have been performed to study the processes in the MBE growth. In an interesting experiment, O. P. Karpenkoa, S. M. Yalisove and D. J. Eaglesham studied the surface roughening during Si(100) homoepitaxial growth by using reflection high energy electron diffraction (RHEED) and transmission electron microscopy (TEM) [18]. Fig. 4.47 shows Bright field, cross-section TEM

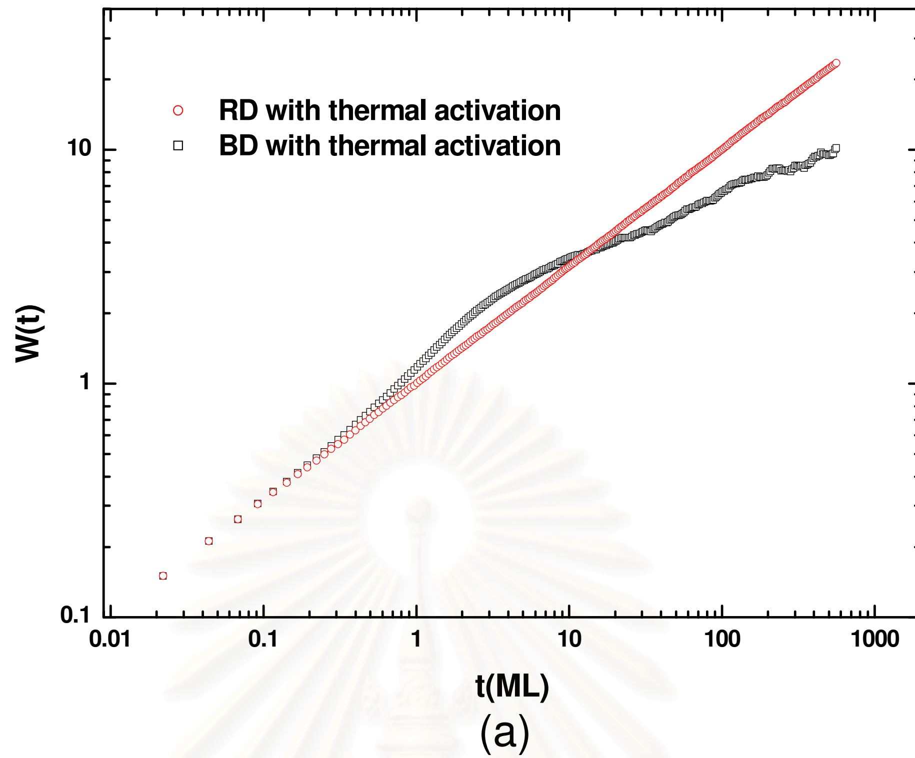

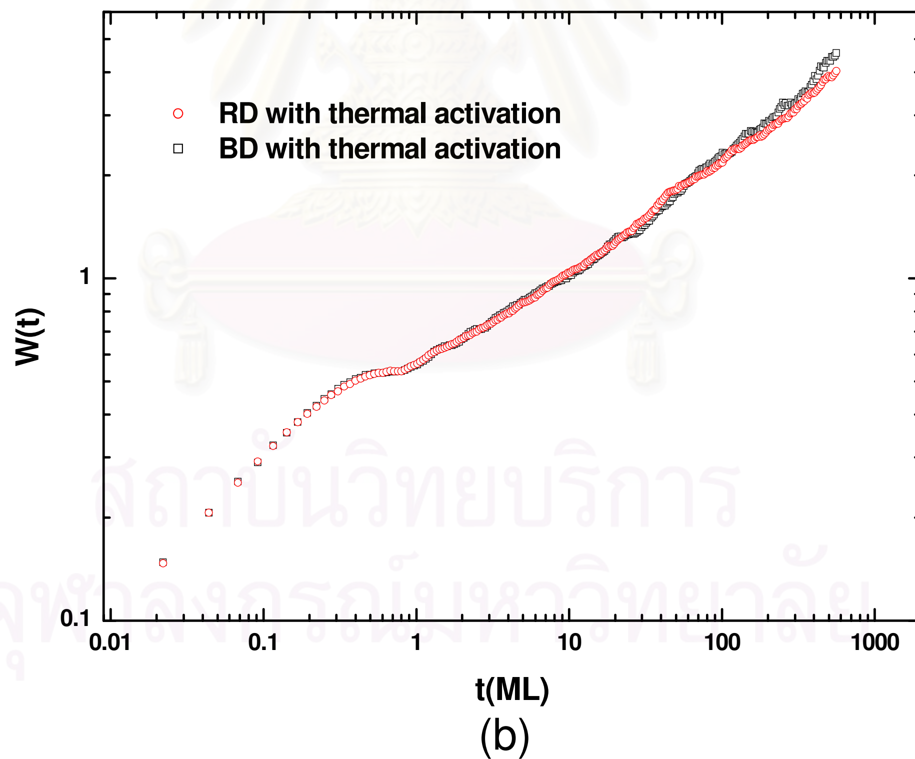

Figure 4.46: Plot of the interface width $W(t)$ versus the growth time t on log-log scale of the BD model with thermal activation model compares with the RD model with thermal activation on the substrate size $L = 500$ at (a) $T = 400$ K and (b) $T = 700$ K.

electron microscopy (TEM) [18]. Fig. 4.47 shows Bright field, cross-section TEM micrograph of a Si (100) homoepitaxial layer grown at $T = 548$ K. They found that the surface roughness increases with deposited thickness and a roughening rate decreases when the growth temperature increases. R. A. Hamm, S. N. G. Chu, R. Hull, L. R. Harriott,and H. Temkin studied homoepitaxial film growth of InP by using atomic force microscope (AFM) and TEM [19]. They observed a smooth morphology of the film at the high growth temperature and the density of defect is strongly dependent on the temperature. The surface roughness increases with the deposited thickness and a roughening rate decreases when the growth temperature increases. W. C. Elliott, P. F. Miceli, T. Tse and P. W. Stephens studied the kinetic roughening during homoepitaxial growth of Ag(111) and Ag (001) by using x-ray reflectivity [20]. They found that the root mean square roughness increases as the power of deposited thickness and the growth exponent decreases when the growth temperature increases. These experiments agree with our discrete models at high substrate temperature that when the substrate temperature increases, the surface becomes smooth. The substrate temperature has an effect on the defect density. The roughness of the film increase as power of the growth time. The growth exponent decreases when the growth temperature increases. In the roughness study, a number of experimental measurements of the growth exponent have been reported for a variety of materials. For example, Joseph E. Van Nostrand, S. Jay Chey, M. -A. Hasan, David G. Cahill, and J. E. Greene studied the homoepitaxial growth of Ge(001) by using scanning tunneling microscopy (STM) [21]. They reported the growth exponent $\beta = 0.32$. F. Wu, S. G. Jaloviar, D. E. Savage, and M. G. Lagally studied kinetic roughening of steps on vicinal Si(001) by using STM [22]. They reported the growth exponent $\beta = 0.29$. H.-J. Ernst, F. Fabre, R. Folkerts, and J. Lapujoulade investigated the growth of a Cu(100) crystal with helium atom beam scattering [23]. They reported the growth exponent $\beta = 0.26$. From these experiments, the growth exponent is reported to be in the $0.2 - 0.4$ range that agrees with our growth exponent at high substrate temperature.

From the study, our discrete models can predict some basic properties of the film but they cannot be compared directly with real growth. One very obvious

reason is that a film is grown on a two dimensional substrate in experiments but our study use one dimensional models. To represent the experiment, the model need to be extended to 2+1 dimension.

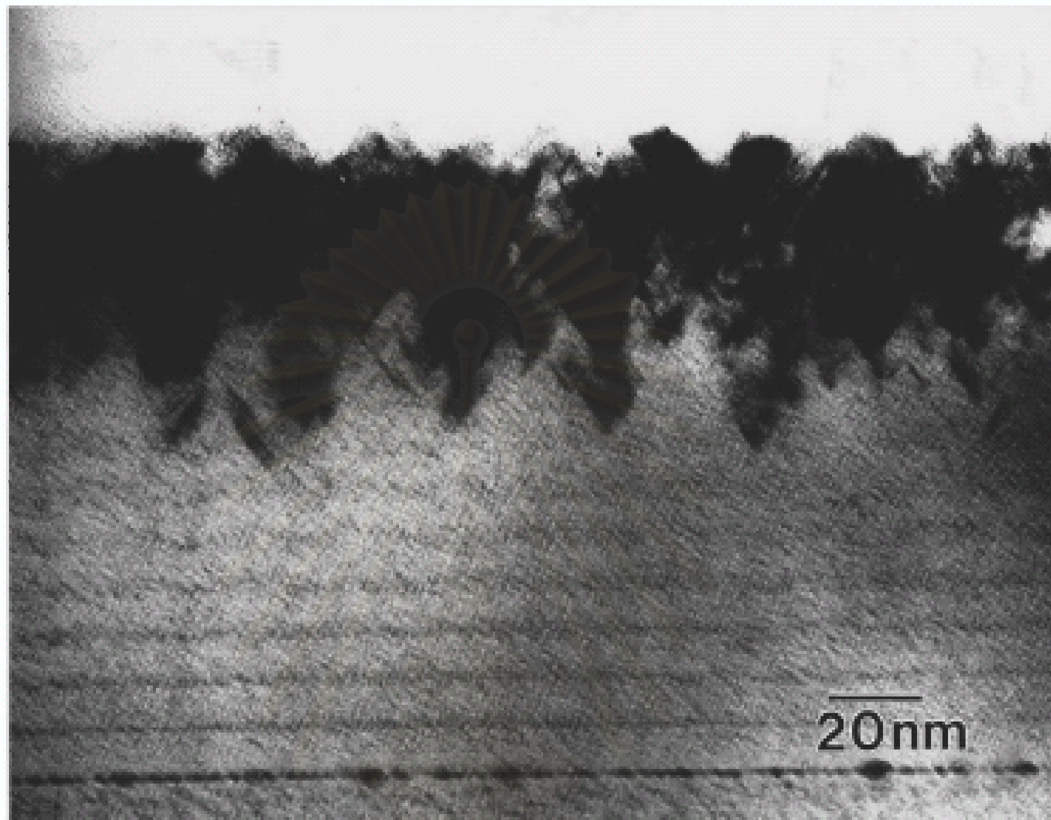

Figure 4.47: Bright field, cross-section TEM micrograph of a Si (100) homoepitaxial layer grown at $T = 548\ K$ [18].

สถาบันวิทยบริการ
จุฬาลงกรณ์มหาวิทยาลัย

CHAPTER V

CONCLUSIONS

In this work, we use two discrete models in $(1 + 1)$-dimension to study homoepitaxial growth of the MBE growth in which void defect can be formed. These discrete models allow overhangs and bulk vacancies in the film. They are Random Deposition (RD) model with thermal activation and Ballistic Deposition (BD) model with thermal activation. In the RD model with thermal activation, the deposition rule obeys Solid-On-Solid (SOS) condition, bulk vacancy, overhanging of an atom and desorption are not permitted. In the BD model with thermal activation, the SOS condition is not restricted. The diffusion process, which is the essential process of MBE, is possible in both models. In the diffusion process, an atom on the surface can move continuously to an empty neighboring site until it is completely bonded by other atoms. The hopping rate is estimated using the Arrhenius expression which depends on the substrate temperature. Since the SOS condition is not applied in this process, void defect can be formed. From the models, we observe the properties of the film affected by the substrate temperature through its morphology, interface width, defect density and height-difference correlation.

For the RD model with thermal activation, we found that the growth of the film can be divided into two main regimes according to the morphology and the defect density. In the first regime, the substrate temperature is low in the range of T less than 600 K. The surface of the film is very rough and the void defect density increases with the substrate temperature. This is because the hopping rate is small. The atom is deposited randomly without any diffusion most of the time. As a result, the film is very rough similar to that of the RD model. When we increase the temperature, the surface atom becomes more probable to

diffuse. Thus, void defect starts forming and density increases with the substrate temperature. The second regime, at high substrate temperature in the range of $T \geq 600$ K, the film becomes smooth and the void defect density decreases as the substrate temperature increases. This is because the surface atom has high a probability to diffuse to search for a suitable site that leads to layer-by-layer growth mode.

From observing the roughness, we found that at low substrate temperature, the plot of interface width with time has the slope β of about 0.5. This β is the same as in the RD model where the height of the film increases independently. The height-difference correlation function $G(r)$ also shows that the height of the film increases independently. This result shows that the roughness tends to increase indefinitely. This is because the surface atom has low probability to diffuse at the low substrate temperature. At higher substrate temperature, the β decreases as the substrate temperature increases. This result shows that the growing rate of the roughness increases slower than in the RD model. This is because the surface atom has high probability to diffuse that leads to layer-by-layer growth mode. The $G(r)$ shows that the surface height does not grow independently because the surface atom can diffuse to the neighboring site and decreases the difference of the neighboring site.

For the BD model with thermal activation, we found that at the low substrate temperature ($T < 600$ K), the surface of the film is rough and the defect density is high. From observing the roughness, the films has the growth exponent β of about 0.26. The height-difference correlation function $G(r)$ shows that the surface height increases with correlating to the neighboring sites. These results is the same in the BD model. This is because the hopping rate is low. The atom is deposited following the deposition rule of BD model in which the bulk vacancy, overhanging of an atom can be created and has small probability to diffuse. As a result, the film shows the same behavior as in the BD model. When the substrate temperature increases, the film becomes smooth and the defect density decreases. The growth exponent decreases as the substrate temperature increases. $G(r)$ show the same behavior as the RD with thermal activation at high substrate temperature. This can be explained that in a system with high substrate temperature,

atom has high hopping rate and can diffuse to rearrange the formation in layer-by-layer mode. As a result, the film has a smooth surface and the defect density decreases.

In this study, the models are applied only in one dimensional system. To make more realistic situation two dimensional system should be considered.

สถาบันวิทยบริการ
จุฬาลงกรณ์มหาวิทยาลัย

References

1. Arthur, J. R. Molecular beam epitaxy. *Surf. Sci.* **500** (2002): L189-L217.

2. Lanczycki, C. J. *Nonequilibrium interface growth: Roughening, coarsening and scale invariance.* Doctoral dissertation, Faculty of the Graduate School, University of Maryland, 1995.

3. Chambers, S. A. Epitaxial growth and properties of thin film oxides. *Surface Science Reports* **39** (2000): 105-180.

4. Das Sarma, S., Lanczycki, C. J., Kotlyar, R., and Ghaisas, S. V. Scale invariance and dynamical correlations in growth models of molecular beam epitaxy. *Phys. Rev. E* **53** (1995): 359-388.

5. Das Sarma, S. Growth models for virtual molecular beam epitaxy. *Computational Materials Science* **6** (1996): 149-151.

6. Wolf, D., and Villain, J. Growth with surface diffusion. *Europhys. Lett.* **13** (1990): 389-394

7. Das Sarma, S., and Ghaisas, S. V. Surface diffusion length under kinetic growth conditions. *Phys. Rev. B.* **46** (1992): 7380-7311.

8. Barabási, A. -L., and Stanley, H. E. *Fractal Concepts in Surface Growth.* Cambridge: Cambridge University Press, 1995.

9. Kohlera, U., Jensena, C., Wolfa, C., Schindlerb, A. C., Brendelb, L., Wolf-bJohn, D. E., Arthur, R. Investigation of homoepitaxial growth on bcc surfaces with STM and kinetic Monte Carlo simulation. *Surf. Sci.* **454-456** (2000): L676-L680.

10. Tamborenea, P. I., and Das Sarma, S. Surface-diffusion-driven kinetic growth on one-dimensional substrates. *Phys. Rev. E* **48** (1993): 2475-2594.

11. Kardar, M. Roughness and ordering of growing films. *Physica A* **281** (2000): 295-310.

12. Meakin, P., Ramanlal, P., Sander, L. M., Ball, R. C. Ballistic deposition on surface. *Phys. Rev. A* **34** (1986): 5091-5103.

13. Elliott, W. C., Miceli, P. F., Tse, T., Stephens, P. W. Temperature and orientation dependence of kinetic roughening during homoepitaxy: A quantitative x-ray-scattering study of Ag. *Phys. Rev. B* **54** (1996): 17938-17942.

14. Das Sarma, S., Ghaisas, S. V., and Kim, J. M. Kinetic super-roughening and anomalous dynamic scaling in nonequilibrium growth models. *Phys. Rev. E* **49** (1994): 122-125.

15. Vvedensky, D. D., Zangwill, A., Luse, C. N., and Wilhy, M. R. Stochastic equations of motion for epitaxial growth. *Phys. Rev. E* **48** (1993): 852-862.

16. Schimschak, M. and Krug, J. Bulk defects and surface roughening in epitaxial growth. *Phys. Rev. B* **52** (1995): 8550-8563.

17. Chanyawadee, S. *Modeling of molecular beam epitaxy growth under Ehrilich-Schwoebel potential barrier.* Thesis, Faculty of Science, Chulalongkorn University, 2004.

18. Karpenkoa, O. P., Yalisove, S. M., and Eaglesham, D. J. Surface roughening during low temperature Si(100) epitaxy. *J. Appl. Phys.* **82** (1997): 1157-1165.

19. Cotta, M. A., Hamm, R. A., Chu, S. N. G., Hull, R., Harriott, L. R. and Temkin, H. Kinetic roughening in Molecular Beam Epitaxy of InP. *Brazilian Journal of Physics* **26** (1996): 75-82.

20. Elliott, W. C., Miceli, P. F., Tse, T., and Stephens, P. W. Temperature and orientation dependence of kinetic roughening during homoepitaxy: A

quantitative x-ray-scattering study of Ag. *Phys. Rev. B* **54** (1996): 17938-17942.

21. Van Nostrand, J. E., Chey, S. J., Hasan, M. -A., Cahill, D. G. and Greene, J. E. Surface Morphology during Multilayer Epitaxial Growth of Ge(001). *Phys. Rev. Lett.* **74** (1995): 1127-1130.

22. Wu, F., Jaloviar, S. G. Savage, D. E. and Lagally, M. G. Roughening of steps during homoepitaxial growth on Si(001). *Phys. Rev. Lett.* **71** (1993): 4190-4193.

23. Ernst, H. J., Fabre, F., Folkerts, R. and Lapujoulade, J. Observation of a growth instability during low temperature molecular beam epitaxy. *Phys. Rev. Lett.* **72** (1994): 112-115.

สถาบันวิทยบริการ
จุฬาลงกรณ์มหาวิทยาลัย

Vitae

Narong Chanlek was born on January 17, 1981 in Samutsongkram, Thailand. He received his bachelor degree of science (second class honor) in physics from Kasetsart University in 2002. He was supported the financial by the Development and Promotion of Science and Technology Talents Project (DPST) during his study.

CONFERENCE PRESENTATION:

2005 N. Chanlek and P. Chatraphorn. Void Defect Formation in A Model for Molecular Beam Epitaxy. 31th Congress on Science and Technology of Thailand, Suranaree University (18-20 October; 2005)

2006 N. Chanlek, P. Chatraphorn. and N. Phaisangittisakul. Effects of Substrate Temperature on Molecular Beam Epitaxy Model with Void Defect Formation. the 10th Annual National Symposium on Computational Science and Engineering 2006, Faculty of Science, Chaing Mai University (22-24 March; 2006)

สถาบันวิทยบริการ
จุฬาลงกรณ์มหาวิทยาลัย